Thesis for the Degree of Doctor of Philosophy

Summer Climate Variability during the Past 1200 Years in Central Scandinavia

– A Tree-Ring Perspective

Peng Zhang

UNIVERSITY OF GOTHENBURG

Faculty of Science

Doctor Thesis A154
University of Gothenburg
Department of Earth Sciences
Gothenburg, Sweden 2015

ISBN: 978-91-628-9476-4
ISSN: 1400-3813

Peng Zhang

Summer Climate Variability during the Past 1200 Years in Central Scandinavia – A Tree-Ring Perspective

A154 2015
ISBN: 978-91-628-9476-4
ISSN: 1400-3813
Internet-id: http://hdl.handle.net/2077/38805
Printed by Kompendiet

Distribution: Department of Earth Sciences, University of Gothenburg, Sweden

To my family for their love and support

ABSTRACT

To set the current 20th century warming in a long-term context, significant efforts have been made to reconstruct hemispheric-to-global temperatures beyond the instrumental period. Tree-rings, which have annual resolution and can be precisely dated, have been widely used to infer past climate variability. In Fennoscandia, tree-ring maximum latewood density (MXD) provides so far the best high-resolution natural archive of summer temperature, and has been used to infer regional temperature variability for the last millennium. However, most of the temperature reconstructions have been based on data from northern Fennoscandia. In central Scandinavia, MXD based temperature reconstructions have not been able to reach the Medieval Climate Anomaly (MCA) when the climate conditions in some regions are analogue to the current warming, but without strong influences from human activities. This is a key period to evaluate if current warming can be reached without anthropogenic influences.

To improve our understanding of past summer climate variability in central Scandinavia, in this thesis work, efforts were made to 1) find Scots pine (*Pinus sylvestris* L.) tree-ring samples from the central Scandinavian Mountains to increase the sample replication before 1750 CE and to extend it over the MCA, 2) examine if tree-ring data can represent annual conditions by comparing annual and summer temperature variability at different timescales in central Scandinavia. The results show that the local tree line in central Scandinavia during the MCA and early Little Ice Age (LIA) was about 140 m higher than at present. The temperature sensitivity of pine growth might be dampened by more humid growth condition. The result implies that temperature reconstructions predominantly based on the tree-ring widths from lake-shores may need to be re-evaluated. Focusing on tree-ring density, it was shown that mean absolute MXD values varied notably with elevation, with higher elevation having lower MXD values due to occurrence of the temperature gradients along altitudes. Heterogeneous temporal distribution of tree-ring samples at different elevations could seriously bias the long-term trend of the temperature reconstruction based on these samples. A mean-adjustment method was developed to overcome this bias. The reconstruction based on unadjusted data yielded 0.4 ℃ lower average warm-season temperature during the period 850-1200 compared to the mean-adjusted reconstruction. The new warm-season (April-September) temperature reconstruction in central Scandinavia covering 850-2011, suggests a MCA during ca. 1000-1100, followed by a transition period before the onset of the LIA proper in the mid-16th century. During the past 1200 years, the late 17th century to early 19th century was the coldest period in central Scandinavia, and the warmest 100 years occurred during the 20th century. The new reconstruction suggests lower temperature during the late MCA (ca. 1100-1220) and higher temperature during the LIA (1610-1850) than the previous reconstruction, and shows regional differences in temperature evolution between northern and central Scandinavia before 1300 CE. Overall colder climate conditions are recorded in central Scandinavia before 1200 CE and warmer conditions during 1200-1300 leading to a mismatch in phase at multidecadal to century timescales before 1300 CE. During 1100-1250, central Scandinavia is dominated by warm, cloudy and wet summer conditions, while during the LIA the region was dominated by cold and sunny summers and partly wet conditions. The transition period between the MCA and LIA (around 1350-1550) was dominated by relatively dry conditions. During this period, temperatures were positively correlated with sunshine hours at multidecadal to century timescales, which was different from MCA and LIA. For central Scandinavia, the summer temperature overall is not a good ‘proxy’ for the annual temperature especially at the 2-16 year timescales.

Keywords: Central Scandinavia, climate variability, dendroclimatology, maximum latewood density, Medieval Climate Anomaly, model-proxy data comparison, *Pinus sylvestris* L., temperature, tree-ring width

PREFACE

This doctoral thesis consists of a summary (Part I) followed by four appended papers (Part II), referred to in the text by Roman numerals. The papers are reprinted with permission from respective journal.

I. Paper I
Linderholm, H.W., **P. Zhang**, B.E. Gunnarson, J. Björklund, E. Farahat, M. Fuentes, E. Rocha, R. Salo, K. Seftigen, P. Stridbeck and Y. Liu (2014), Growth dynamics of tree-line and lake-shore Scots pine (*Pinus sylvestris* L.) in the central Scandinavian Mountains during the Medieval Climate Anomaly and the early Little Ice Age. *Frontiers in Ecology and Evolution: Paleoecology* 2: 20. doi: 10.3389/fevo.2014.00020.

P. Zhang collected and prepared the data, conducted the data analysis, visualized the results, and contributed to the writing.

II. Paper II
Zhang, P., J. Björklund and H.W. Linderholm (2015), The influence of elevational differences in absolute maximum density values on regional climate reconstructions. *Trees*: 1-13. doi: 10.1007/s00468-015-1205-4.

P. Zhang initiated the paper, prepared the data, conducted the analysis, visualized the results, and contributed to the bulk of the writing.

III. Paper III
Zhang, P., H.W. Linderholm, B.E. Gunnarson, J. Björklund and D. Chen (2015), 1200 years of warm-season temperature variability in central Fennoscandia inferred from tree-ring density. *Climate of the Past Discussion*, 11, 489-519, doi:10.5194/cpd-11-489-2015 (Revised and resubmitted to *Climate of the Past*)

P. Zhang initiated the paper, prepared the data, conducted the analysis, visualized the results, and contributed to the bulk of the writing.

IV. Paper IV
Zhang, P., D. Chen, H. Linderholm and Q. Zhang, How similar are annual and summer temperatures in central Sweden?-Perspectives from observations, model simulations and tree-ring density (To be submitted to *Advances in Climate Change Research*)

P. Zhang collected the data, conducted the analysis, visualized the results, and contributed to the bulk of writing.

A peer reviewed paper not included in the thesis:

Björklund, J., B. E. Gunnarson, K. Seftigen, **P. Zhang** and H. Linderholm. Using adjusted Blue Intensity data to attain high-quality summer temperature information: A case study from Central Scandinavia (2014), *The Holocene* 1-10, doi: 10.1177/0959683614562434**.**

Table of Contents

I. Summary

II. Papers I-IV

Part I

Summary

1. Introduction

1.1 The importance of studying the regional temperature variability

In order to assess the magnitude of the 20th century warming (e.g. Parmesan and Yohe, 2003) in a historical context, climate scientists have put big efforts into exploring the temperature variability during the past millennium (Mann et al., 1999). With the completion of a series of paleoclimate reconstruction projects (e.g. Millennium (McCarroll et al., 2013), PAGES 2k (PAGES 2k Consortium, 2013)), temperature variability during the last millennium has been reconstructed at continental and hemispheric scales based on a huge number of proxy data (e.g. Jones et al., 2001; Ljungqvist, 2010; Moberg et al., 2005). Together with the temperature simulations from climate models, proxy reconstructions describe the general profile of the large-scale temperature evolution, which is dominated by three distinguished temperature regimes: the Medieval Climate Anomaly (MCA, 950-1250 (Lamb, 1969; Grove and Switsur, 1994)), the Little Ice Age (LIA, 1450-1850, (Schneider and Mass, 1975; Grove, 2001)) and the 20th century warming (20C, 1900-present) (IPCC, 2013). However, regional reconstructions show different onsets and timings of the three temperature regimes, highlighting the spatial variability in climate (Ljungqvist et al., 2012; PAGES 2k Consortium, 2013). Identifying local and regional scale climate changes is highly important for human society regarding the impacts on economy and safety (Patz et al., 2005), and this information can be directly useful in making climate adaption policies (Adger et al., 2005). Temperature reconstructions at regional scales are also important, since they can provide data to improve our understanding of the temperature changes and the physical mechanism under natural forcing conditions (Steinhilber et al., 2012), and can also provide better spatial coverage for improving the accuracy of large-scale temperature reconstructions. At regional scales, high-resolution proxies, such as tree-rings, can be used to investigate temporal and spatial variability of climate extremes in their magnitude, frequency and return periods (e.g. Esper et al., 2001, Esper et al., 2012).

Central Scandinavia is a region located in the northern hemisphere high latitudes, and likely affected by the 'polar amplification' (an enhanced warming or cooling phenomenon at polar region due to feedback mechanisms such as sea ice and snow cover feedbacks (Holland and Bitz, 2003)). Thus, the temperature changes in this region during the last millennium are easier to identify than most of the regions at low latitudes. Central Scandinavia is also a region strongly influenced by the atmospheric and ocean circulation. Previous studies have shown that the North Atlantic Oscillation (NAO) (Hurrell, 1995) has an important effect on the regional temperature variability on monthly and interannual timescales (Chen and Hellström, 1999). In summer, the Summer North Atlantic Oscillation (SNAO) exerts a strong influence on temperature, precipitation and cloudiness in this region through changes in the position of the North Atlantic storm track (Folland et al., 2009). Due to the proximity to the Norwegian Sea, this region is also affected by North Atlantic sea-surface temperature (SST) (Rodwell et al., 1999; Rodwell and Folland, 2002). The leading mode of Atlantic SST (the Atlantic Multidecadal Oscillation, AMO (Kerr, 2000)) has been found to have strong impacts on the temperature variability in this region at multidecadal to century timescales (Sutton and Dong, 2012). The temperature variability in this region during the last millennium has been strongly influenced by atmospheric circulation changes caused by natural forcings (i.e. changes of solar radiation and volcanic eruptions) (Shindell et al., 2001; 2003) and internal variability (i.e. the stochastic changes of circulations such as NAO and AMO without influences of external forcings) in the climate system (Goosse et al. 2005; Servonnat et al. 2010; Goosse et al., 2012). Thus, this region provides an excellent platform to study the mechanisms of climate changes under natural and anthropogenic conditions during the preindustrial period and the recent 150 years.

Scandinavia is an excellent region for regional climate change research not only because it is a region having some of the longest meteorological records in the world (Moberg et al., 2002), but also due to its large tracts of boreal forest which enable high-resolution tree-ring based temperature reconstructions far back in time. However, most of the work that has been done regarding high-resolution reconstructions of the late Holocene has mainly been from northern Fennoscandia. Since previous studies have shown that there could be differences on regional temperature evolution (PAGES 2k Consortium, 2013), it is important to extend the temperature reconstruction further south, such as Central Scandinavia. This will improve our understanding of the temperature variability in the whole Scandinavia, but also further our understanding of spatial differences in the temporal evolution of late Holocene temperatures.

1.2 The late Holocene temperature variability

Our present knowledge of late Holocene climate variability in central Scandinavia comes from various paleoclimate reconstructions. These reconstructions are mainly based on natural archives, called proxies, which record various environmental and climate parameters. Regional climate variability has been inferred from lake sediments, speleothems, peat sequences and tree-ring data. However, all proxy data have their limitations in terms of the strength of the climate signal and its resolution (see Table 1.1 that summarizes the features of the most commonly used paleoclimate proxies in central Scandinavia). Lake sediments and speleothems have been used to infer July and annual mean temperature during the Holocene in central Scandinavia (Hammarlund et al., 2004; Sundqvist et al., 2010; Seppä et al., 2009, see Figure 1.1 for the location of the sites).

Pollen grains and insects such as chironomids that were washed or blown into lakes can accumulate in lake sediments, and provide a record of past vegetation and living environments of insects, which can be used to infer the variability of past climate. Speleothems are mineral deposits formed from groundwater in underground caverns. These cave deposits, which come in form of stalagmites and stalagtites, can be radiometrically dated, and the thickness of depositional layers or isotopic records can be used to infer past climate conditions. Although these proxies successfully reproduce the low-frequency temperature variability for long-time periods (several millennia), the relatively low resolution limits our understanding of the temperature variability at annual to century timescales.

Due to the extensive occurrence of trees close to the tree-line in the central Scandinavian Mountains, where the annual growth is closely linked to summer temperatures, and also due to the high temporal resolution (annual resolution) and exact dating of the tree-ring data (where each tree ring can be assigned an calendar year), tree-ring data has been widely used to reconstruct past regional temperature variability (Linderholm et al., 2010). The earliest research using tree rings as proxies for climate (dendroclimatology) in this region dates back to the year of 1936 (Erlandsson, 1936). In 1970s, Fritz Schweingruber and colleagues collected *Pinus sylvestris* L. (Scots pine) tree-ring samples from historical buildings as a part of a grand sampling strategy to create a dense tree-ring network from cool moist regions across the Northern Hemisphere (Schweingruber et al., 1990). This data has been included in temperature reconstructions of local (Gunnarson et al., 2011) and Hemispheric scales (Esper et al., 2002; D’Arrigo et al., 2006). In the mid-1990s, work started on building a multi-millennial long pine tree-ring chronology which could reflect summer temperature variability in this region for large parts of the Holocene. This was to be a southern complement to the >7000 year-long tree-ring records from northernmost Fennoscandia in Torneträsk (Briffa et al., 1990, 1992; Grudd et al., 2002) and Finnish Lapland (Helama et al., 2002). Tree-ring samples were collected from living and dead trees. Here living pines can reach ages of up to 700 years, but to extend the tree-ring record back in time, large quantities of dead pines, preserved for centuries to millennia found in small mountain lakes were used (Gunnarson, 2001; Gunnarson and Linderholm, 2002). Based on these samples, a tree-ring width chronology was built spanning the period from 4868 BCE to 2006 CE with two minor gaps near 1600 BCE and 900 CE and one larger gap near 2900 BCE. This data was subsequently used to reconstruct summer temperatures back to 1600 BCE (Linderholm and Gunnarson, 2005). In addition, the temporal distribution patterns of the wood found in the mountain lakes (called subfossil wood) was used as an indicator of regional humidity fluctuations (Gunnarson et al., 2003; Gunnarson, 2008).

Figure 1.2 shows the temperature variability inferred from different natural archives during the last millennium. The tree-ring records show a much higher temporal resolution than the lake sediments or sometimes speleothems. Mean July temperature was inferred from the number of chironomid head capsules buried in the different layers of the Spåime lake sediment, and the radiocarbon dating technology used to estimate the time interval of the formation of each layer (Hammarlund et al., 2004). Annual mean temperatures were inferred from the $\delta^{18}O$ record of a stalagmite collected from Korallgrottan (Sundqvist et al., 2010), and the number of pollen grains in the sediment of lake Klotjärnen, Svartvatnet and Tiåvatnet (Seppä et al., 2009). The chironomid based mean July temperature reconstruction indicates an overall cooling trend from the MCA to LIA, followed by a slight warming trend from the 16th century to early 20th century. It clearly shows multi-century-timescale temperature variability, but the variability in the higher frequency domain is totally missing. The pollen based annual and mean July temperature reconstructions seem to have higher time resolution, but still, the resolution is not enough for analysis at interannual to century timescales. The mean July temperature reconstructions from Svartvatnet and Tiåvatnet both show a warming trend during the last millennium, which differs from the other reconstructions (see Figure 1.2). This could be due to the coastal location of the two lakes. The $\delta^{18}O$ record from Korallgrottan shows temperature variability at higher timescales than the pollen and chironomid based records. However, the variance in the stable isotope series is much smaller at multi-decadal to century scales than that at multi-century scales. Although the multi-decadal variability seems to be recorded, the coarse dating still limits our understanding of the climate conditions at decadal timescales. The annually resolved tree-ring records provide information of temperature variability from annual to multi-millennia timescales, but can only provide the temperature information for the growing season (mainly in summer).

Table 1.1 Temporal resolution, range and potential information of natural archives used for the climate reconstructions in central Scandinavia (Bradley, 1999)

Archive	Temporal resolution	Temporal range (years)	Potential information derived
Tree rings	Annual	~ 10^4	T, P, B, V, S
Lake sediments	~ Annual to decadal	~ 10^5	T, B, P, V, C
Pollen	~ Decadal to centennial	~ 10^5	T, P, B
Speleothems	~ Annual to centennial	~ $5*10^5$	C, T, P
Peat sequences	~ Decadal to centennial	~ 10^4	P

T = temperature; P = precipitation, humidity, or water balance; C = chemical composition of air or water; B = information on biomass and vegetation patterns; V = volcanic eruptions; S = solar activity

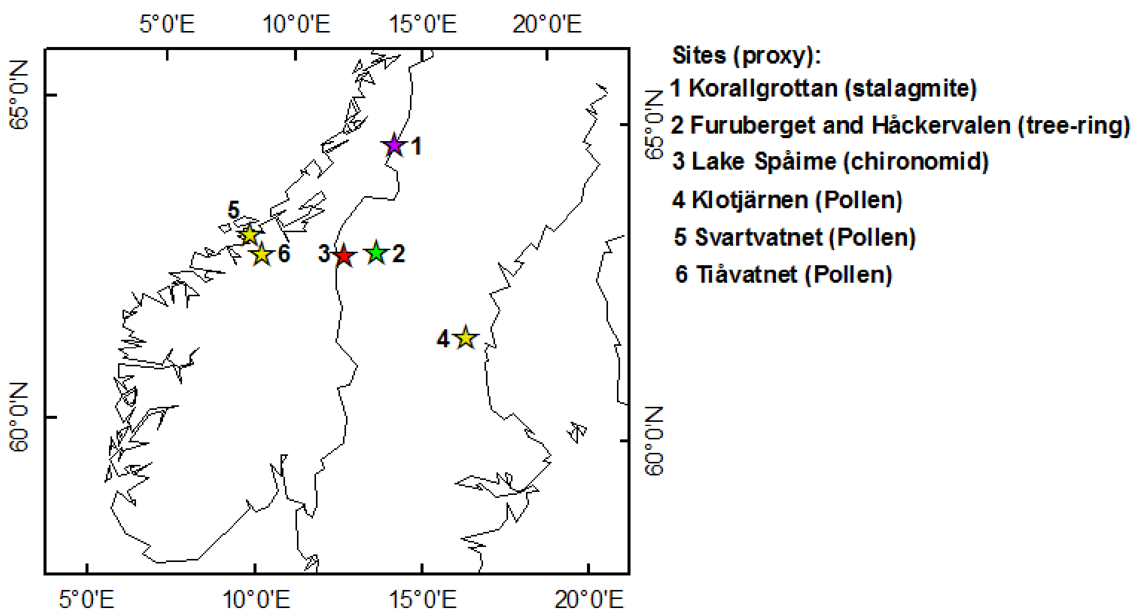

Figure 1.1 Map of central Scandinavia. Green, red, purple and yellow stars mark the locations of tree-ring (Linderholm and Gunnarson, 2005; Gunnarson et al., 2011), lake sediments (Hammarlund et al., 2004), stalagmite (Sundqvist et al., 2010) and pollen (Seppä et al., 2009) sampling sites. These samples were used to infer the temperature variability in central Scandinavia back in time in previous studies.

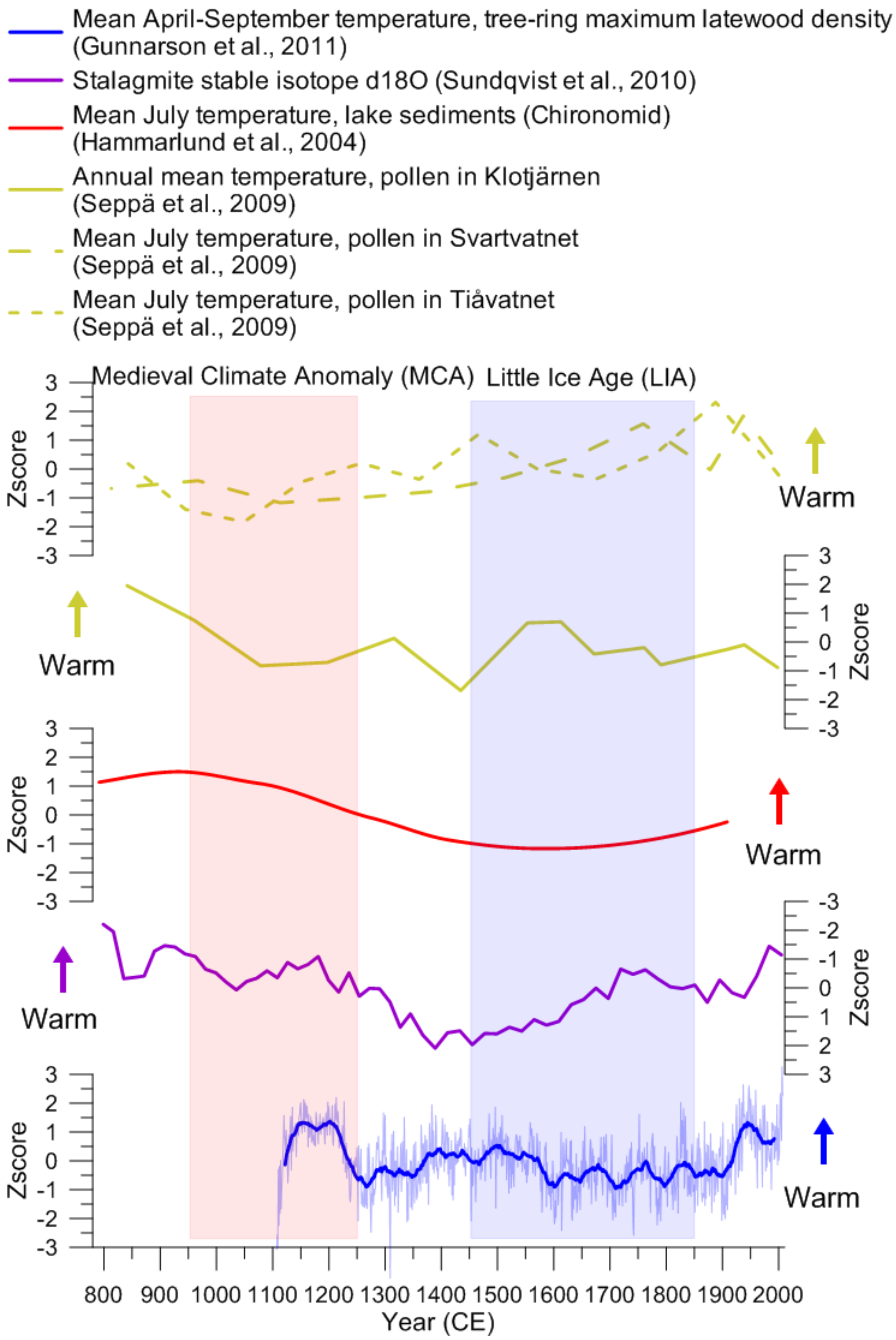

Figure 1.2 Six temperature reconstructions for central Scandinavia based on tree-ring, lake sediment, speleothem and pollen data. MCA and LIA are indicated with light red and light blue shadings. All records were normalized for comparisons. The tree-ring based reconstruction was smoothed with 31-year moving average.

1.3 Statement of the problem

Medieval Climate Anomaly (MCA) is a period when the climate conditions in some regions are analogue to current warming, but without strong influences from human activities (Mann et al., 2009). This is a key period to evaluate if current warming can be reached without anthropogenic influences (Crowley and Lowery, 2000; Broecker, 2001). However, there are few high-quality, annually resolved temperature reconstructions covering the MCA in the world (Mann et al. 2008; Pages 2k consortium, 2013). In Fennoscandia, tree-ring maximum latewood density (MXD) provides the best natural archive of summer temperature, and has been used to infer regional temperature variability for the last millennium (Helama et al., 2014; Esper et al., 2014; Matskovsky and Helama, 2014). However, most of the temperature reconstructions have been based on data from northern Fennoscandia (Esper et al., 2012; Melvin et al., 2013). In central Scandinavia, tree-ring data has shown excellent potentials on reconstructing the warm-season (April-September) temperature back to several millennia ago (Linderholm and Gunnarson, 2005; Gunnarson et al., 2011). So far, the MXD based temperature reconstruction for central Scandinavia was not covering the MCA due to the lack of samples during this period.

Previous temperature reconstructions with annual resolution in central Scandinavia have been based on both tree-ring widths and density. However, the tree-ring width based temperature reconstruction covering the period 1632 BCE to 2002 CE have low sample replication in the 9th, 13th and 14th centuries and a gap between 887 CE and 907 CE (Linderholm and Gunnarson, 2005), making it difficult to assess the MCA in this region. A significant improvement was made when tree-ring density data was used to reconstruct the warm-season temperature in this region (Gunnarson et al., 2011, henceforth referred to as G11). However, since this reconstruction only covered the last 900 years (1107-2006), the MCA could not be fully investigated. Moreover, most of the samples before 1750 CE were derived from historical buildings (e.g. churches). Since the geographical origin of the historical samples is unclear, the climate information in the original dataset may be ambiguous (Gunnarson et al., 2011), making it difficult to fully assess the validity of the reconstructed temperature variability especially before 1300 CE.

In this context, a tree-ring maximum latewood density based warm-season (April-September) temperature reconstruction must be extend to at least covering the past 1200 years using the tree-ring samples collected from tree-line areas, in order to assess the magnitude of the 20th century warming compared with the MCA.

2. Aim and objectives

The main aim of this thesis work was to improve the understanding of regional summer climate variability from the MCA to the present in central Scandinavia.

The specific objectives of this thesis work were:

1). Find tree-ring samples from the central Scandinavia Mountains covering the MCA, and increase the sample replication before 1750 CE to replace the samples collected from historical buildings;

2). Reconstruct warm-season (April-September) temperature variability during the past 1200 years in central Scandinavia using tree-ring maximum latewood density;

3). Examine the relationship between annual and summer temperature variability at different timescales in central Scandinavia, using observational data and tree-ring data, and evaluate the performance of climate models on reproducing this relationship.

The works related to the first objective are addressed in Paper I, where growth dynamics of tree-line and lake-shore Scots pine in the central Scandinavian Mountains were analyzed and compared to each other during the MCA and the early LIA.

The second objective is realized in Paper II and Paper III. Due to the heterogeneous geographical distribution of the tree-ring samples in different periods, where samples covering MCA were found at higher elevation, a bias in the final tree-ring density chronology was found if the chronology was produced using a traditional dendroclimatological reconstruction methods. This problem, which has not been previously addressed, is dealt with in paper II, where a mean-adjustment method was developed to overcome this issue. In Paper III, warm-season (April-September) temperature variability was reconstructed using the new tree-ring density chronology.

The third objective is addressed in Paper IV, where the relationship between annual and summer temperature variability was investigated at interannual to century timescales using observational temperature data. A climate model: HadCM3 was evaluated on its performance on reproducing the annual and summer temperature relationship, and on reproducing the variance of annual and summer temperature at the different timescales.

3. Data and methods

3.1 Dendroclimatology

Dendrochronology is the science of dating events such as forest fires, volcanic eruptions, insect attacks and climate events based on the analysis of patterns from tree rings (Fritts, 1976). The subfield dendroclimatology is the science of reconstructing past climate variability using tree rings (Fritts, 1976). The temperature reconstruction in this thesis work is based on the theory of dendroclimatology. Hence, the basic theory of dendroclimatology is addressed in this section.

3.1.1 Sampling strategy and climate signal in tree-rings

Tree growth, which can be described by parameters such as tree-ring widths or cell density, is affected by certain conditions in the forest environment, which provide a basis of the link between climate and tree-ring growth. Temperature, water, light, and soil minerals comprise environmental conditions which are the most common factors influencing tree growth. Depending on where the trees grow, single environmental parameters can determine the annual growth of trees. According to the principle of limiting factors, tree growth cannot proceed faster than is allowed by the most limiting factor (Fritts, 1976). Thus, the growth of trees in arid areas is depending on the availability of water, while trees growing in cold environments are more sensitive to temperature variations. The closer the tree is growing to its species-specific distribution limit, the stronger the influence of climate will be. Hence, in order to infer the past temperature variability using tree-ring proxies, it is crucial to collected tree ring samples from the trees whose growth is mainly limited by temperature variability (Cook, 1990).

High altitude (tree line) and high latitude (subarctic) regions are usually considered to be places where temperature is the main limiting factor for tree growth (Schweingruber et al., 1990). Every year, when the temperature increase to a certain level, the growing season starts, and the cambium start to be active to produce new wood cells. The number, size and density of these wood cells depend on that if the tree has a growth-favorable environment. Sufficient light, water and temperature will benefit the tree growth, and facilitate the formation of more and bigger wood cells and denser cell walls (Fritts, 1976). Usually, during the growing season, the environmental factors in a pine forest can reach the requirement of tree growth. However, in high altitude tree-line areas, the tree growth will be more sensitive to temperature (e.g. Erlandsson, 1936; Linderholm and Gunnarson, 2005), because the temperature in these areas may just reach slightly above those required for tree growth. A decrease in temperature will be expressed by a narrow tree ring.

Central Scandinavia belongs to the northern hemisphere boreal zone. Scots pine, *Picea abies* (L.) H. Karst. (Norway spruce) and *Betula pubescens* Ehrh. (Mountain birch) are the three dominant tree species in this region. Large amounts of Scots pine and Norway spruce having lived thousands of years ago have been found in many small mountain lakes. These samples have been used to build a multi-millennia scale tree-ring width chronology. However, as mentioned before, there are still periods when only few samples are found. The Norway spruce samples preserved in mountain lakes in this region has been recently studied, and used to build a millennium long tree-ring chronology (Rocha, 2014). The mountain birches have also been recently studied for their dendroclimatological potential (Young et al., 2011). In this thesis work, Scots pine was the targeted species.

3.1.2 Cross-dating of tree rings

To build a millennium-long chronology, tree-ring samples from both living and dead trees are needed, since living trees rarely reach ages above 500 years. Dead trees lying on the ground can be persevered for more than 1000 years (Linderholm et al., 2014a), and dead trees buried in lake sediments can be preserved for thousands of years (see Gunnarson, 2008). Together these trees can be used to infer the temperature variability information far back in time. However, the exact year of each ring of a dead tree sample must be confirmed in order to build a continuous tree-ring chronology from different sources.

Cross-dating is the process of dating the calendar year of each individual tree-ring (Wigley et al., 1987). In this process, living trees were initiatively used as references to date dead trees, since we know the exact year of the formation of each ring for a living tree by counting the number of rings from the outermost ring (formed at present year). The tree-ring growth pattern (expressed as the interannual variability of a tree-ring series such as a ring width series) of undated samples are compared to dated samples in a running time window. If the correlation between the two series passes statistical test such as the student’s *t*-test (Baillie & Pilcher, 1973), the calendar year of each ring of the undated sample will be confirmed. Potential dating problems of the individual TRW series were then detected using the COFECHA software (Holmes, 1983), which compares the absolute date to its mean chronology. After dating a dead tree, then this dated dead tree can be used as a reference to date other dead tree samples.

3.1.3 Standardisation techniques

Standardisation is a basic and necessary procedure in dendroclimatology. The basis of this process is that tree-ring widths vary not only due to influences of the environment and climate, but also because of systematic changes in tree age, height, and conditions and productivity of the site (Schweingruber, 1996). We call these non-climatological growth expressions compare to the climate signal we want to extract. In order to preserve the temperature signal as much as possible without distortion from other signals, the non-climatological growth expressions (non-climatic signal or noise) must be removed (Cook, 1985).

Consider a tree-ring series as a linear aggregate of climate signals and non-climatic signals, the non-climatic signal first needs to be estimated, and then removed from the tree-ring series. The non-climatic signals contain 1) age related trend, 2) disturbance pulse caused by a local endogenous disturbance, 3) disturbance pulse caused by a stand-wide exogenous disturbance, and 4) the largely unexplained year-to-year variability not related to any other signals (Cook and Peters, 1981). The age related trend reflects the geometrical constraint of adding a volume of wood to a stem of increasing radius, thus usually exhibit an exponential decay as a function of time (Fritts et al., 1969; Cook and Kairiukstis, 1990). The endogenous disturbances are related to natural stand competitions, where individual trees can be disturbed by expressing as suppression and release in tree-ring widths. When the size of a forest is sufficiently big, these disturbances can be seen as random events. The exogenous disturbances can be seen as common non-climatic stochastic signals which usually represent disturbances from events such as fire, insect outbreaks or logging which cannot be removed in the standardisation procedure but might be minimized by a careful site selection (Fritts, 1976).

Generally, non-climatic signals and especially age-related trends are represented by a fitted least square negative exponential function, a polynomial or spline model (Fritts, 1976), which is divided or subtracted from each raw tree-ring measurement to obtain dimensionless indices for building the chronology. This approach is widely used, but it severely limits the attained variability of long chronologies that are based on multi-generation datasets, because all indices have similar averages, referred to as the ‘segment length curse’ (Cook et al., 1995; Briffa et al., 1996).

This limitation can be overcome by quantifying the non-climatological growth expression as an average of the whole sample aligned by cambial age, again represented with a single mathematical function. Subsequently this single function is subtracted from each individual tree-ring measurement. This method is called as Regional Curve Standardisation (RCS; Briffa et al., 1992). By using one single function for all tree-ring series, the drawback is that less unwanted mid-frequency variability is removed in order to be able to preserve the low-frequency (>segment length) variability (Melvin, 2004), along with possible trend distortion described in (Melvin and Briffa, 2008).

Alternatively, the non-climatological expression in tree-ring data can be quantified with the signal-free approach to standardisation described in Melvin and Briffa (2008). This can be done on individual trees (individual signal-free) or as an average of all trees (signal-free RCS). In signal-free RCS chronologies, this can alleviate possible trend distortion, but little noise from stand competition etc. is removed (Melvin and Briffa, 2014 a and b). Björklund et al. (2013) recently developed a standardisation method called regional curve adjusted individual signal-free approach (RSFi). This method firstly applies the signal-free individual fitting approach (Melvin and Briffa, 2008) to find a unique signal-free curve to fit each individual MXD series. Then, the mean level of each signal-free curve was adjusted by adding or subtracting a constant to have a same mean as the cambial-age segment of the regional curve (RC) of each sample. Different from other RCS methods which use a common curve or multiple curves to estimate the non-climatic signals for all series, the RSFi removes the noise at individual tree level.

3.1.4 Assessing climate signal in tree rings

A tree-ring chronology is subsequently built by averaging each individual standardised tree-ring series. The chronology is then statistically compared to climate variables, such as temperature and precipitation, to explore the growth-climate relationship (Cook and Kairiukstis, 1990). The relationship can be quantitatively estimated by the correlation coefficient between a chronology and a climate variable time series. However, we must make a hypothesis that the same stable relationship between tree growth and the climate variable also occurred in the past (uniformitarian principle, Fritts, 1976).

3.2 Wavelet analysis and EEMD decomposition

Wavelet analysis which is also called wavelet transform is a mathematic method to analyze time series. Using a function called wavelet basis function, this method can decompose a time series into the time-frequency space. Therefore, one is able to determine both the dominant modes of the series variability at each frequency domain and also how those modes vary over time (Torrence and Compo, 1998). This method has been widely used in the geophysics studies for identifying climate signals (e.g. Weng and Lau, 1994). In this thesis work, we used this method to detect the power of the temperature variance at different frequency bands and at different time intervals. The most commonly used Morlet wavelet basis function was used in the temperature series analysis.

Traditional comparison between two time series is to compare the interannual variability and trend (Santer et al., 2000). In this thesis work, the relationship between annual and summer temperature variability was investigated at different timescales. This is similar to a coherency analysis, but the difference is that here the time series are firstly decomposed into the series of different timescales (called frequency bands), and then the relationship between two decomposed series are further investigated. The advantage of this method is that we can directly compare the signals at different timescales and also investigate the dynamic of the signals in its magnitude and phase. The ensemble empirical mode decomposition (EEMD) method (Wu and Huang, 2009) was used to decompose the original time series into different timescales.

EEMD is built on Empirical Mode Decomposition (EMD). EMD is an adaptive time-frequency data analysis method. Using this method, a data generated with nonlinear and nonstationary process can be decomposed into a series of empirical modes and a residual. Each of the empirical modes, defined as an intrinsic mode function (IMF), was sifted out using a iteration process when it satisfying the following conditions: (1) in the whole data set, the number of extrema and the number of zero-crossings must either equal or differ at most by one; (2) at any point, the mean value of the envelope defined by the local maxima and the envelope defined by the local minima is zero (Huang et al., 1998). This method is adaptive and posteriori, so the mode components reflect intrinsic scale characteristics of the original data, and have physically meaningful interpretations (Huang et al., 1998). However, a major drawback of this method is that an IMF which is supposed to reflect the variation at one characteristic scale often consists of signals of widely disparate scale, or a characteristic scale resides in different IMF components (Wu and Huang, 2009). This will weaken the characteristic scale in each IMF. The EEMD is a method further developed from EMD, which overcome the scale separation problem. In this method, the original data is preprocessed by adding white noise, and then is decomposed into IMFs. This step is repeated many times. The ensemble means of the corresponding IMFs were the final IMFs. Both EMD and EEMD methods have been widely used in geophysical studies (Huang and Wu, 2008; Ji et al., 2014).

3.3 Chronology evaluation and reconstruction techniques

Expressed population signal (EPS) was used to test the robustness of the chronology. An EPS value represents the percentage of the variance in the hypothetical population signal in the region that is accounted for by the chronology, where EPS values greater than 0.85 are generally regarded as sufficient (Wigley et at., 1984). The EPS value is closely related to the inter-series correlation and the number of the samples. Higher inter-series correlation and more samples yield higher EPS values.

In order to reconstruct past climate conditions, the direction and strength of the relationship between the tree-ring MXD chronology and observed climate variables must be evaluated. This evaluation is usually referred to as calibration in which a quantitative relationship was given.

Typically the observational data were divided into two parts with the same or similar length. The calibration was conducted based on one part, and then validated based on the other part (Gordon et al., 1982). Then the calibration was done again but based on the other part, and validated based on the first part. The rationale of this processing is to test if the relationship between the chronology and the climate variable is stable along the time. The reduction of error statistic (RE) and coefficient of efficiency (CE) were used to examine reconstruction quality. RE has a possible range of $-\infty$ to 1, and an RE of 1 can be achieved only if the prediction residuals equal zero. Zero is commonly used as a threshold, and the positive RE values in the both calibration periods suggests that the new reconstruction has some skills. Similar to RE, CE is a measure to evaluate the model under the validation period. Values close to zero or negative suggests that the reconstruction is no better than the mean, whereas positive values indicate the strength and temporal stability of the reconstruction.

3.4 Fieldwork

Fieldwork for this thesis work is conducted in the eastern side of the main divide of the central Scandinavian Mountains between 63°N and 63.5°N. The region belongs to the northern boreal zone. The main topography ranges from 800 to 1000 m a.s.l., but scattered alpine massifs to the south reach approximately 1700 m a.s.l. There is a distinct climate gradient in the area. East of the Scandinavian Mountains, climate can be described as semi-continental. However, the proximity to the Norwegian Sea, lack of high mountains in the west, and the east–west oriented valleys allow moist air to be advected from the ocean, providing an oceanic influence to the area(Johannessen, 1970; Johansson and Chen, 2003; Bojariu and Giorgi, 2005). Glacial deposits dominate the area, mainly till but also glacifluvial deposits, peatlands and small areas of lacustrine sediments (Lundqvist, 1969). The forested parts in the central Scandinavian Mountains are dominated by Scots pine, Norway spruce and Mountain birch. Although large-scale forestry have been carried out in most parts of the county, the human impact on trees growing close to the tree line is limited, which is valuable in tree-ring based climate reconstructions (Gunnarson et al., 2012). Figure 3.1 are the pictures taken during the fieldwork at Furuberget and Håckervalen, which shows the environment of the sampling sites.

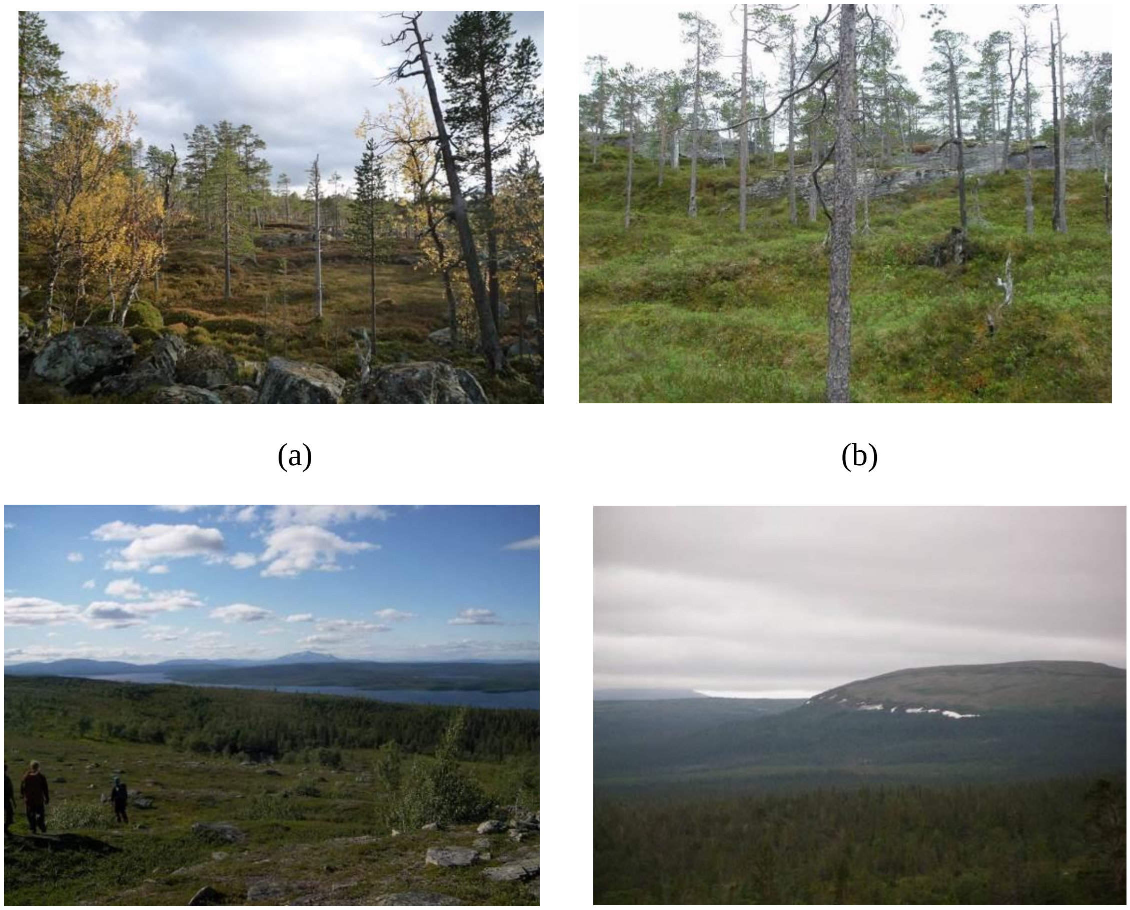

(a) (b)

(c) (d)

Figure 3.1 Pictures showing the environment of the study area: (a) and (b) are taken at Furuberget; (c) and (d) are taken at Håckervalen; (c) shows the above-tree-line environment, and (d) shows the tree line of Gestvalen.

Previous studies have indicated that climate induced lake level fluctuation can influence the number of trees close to the lake shore in central Scandinavia (Gunnarson, 2008). Absence of subfossil samples thus implicates periods with high lake levels, which usually represents a large spatial hydrological change. Due to the wet climate conditions, it is difficult to find subfossil samples in this region which can cover the gap in tree-ring data during the 9th century, and increase the sample depths of 13th and 14th centuries. The reason of lack of samples during these periods could also be due to tree's regeneration pattern (Zachrisson, et al., 1995; Gunnarson and Linderholm, 2002) or due to the preserving matters (e.g. samples were collected as firewood). Although fieldwork in the central Scandinavian Mountains started around 20 years ago, there were still periods when no samples have been found. During 2011-2013, multiple fieldwork campaigns were conducted in this region. The main aim of the fieldwork was to explore new sites to look for samples which could be used to extend G11. Figure 3.2 shows the pictures taken during the fieldworks.

(a) (b) (c) (d) (e) (f)

Figure 3.2 Pictures taken in the fieldworks: (a) dead trees in a lake; (b) dragging a tree from the lake; (c) dead trees dragged out from the lake; (d) after cutting a disc from a dead tree; (e) sampling from a dead tree above present tree line; (f) sampling from a living tree growing at a cliff.

Collection of dead trees from tree-line areas and mountain lakes was the main focus during the fieldworks. Parts of the samples could not be dated with the previous tree-ring chronology, suggesting that they could be too old to be dated with the present chronology. Also, some of the samples from the lakes were from spruce, and these were used to build a millennium-long tree-ring width chronology (Rocha, 2014). Samples covering the 9th century gap were finally found close to the top of the mountain Håckervalen, at ca. 100 meters above the present tree line. These samples, together with samples from Furuberget and the mountain lakes, cover the 8th-18th century, providing enough samples not only to extend and enhance (by increasing the sample depth) the previous temperature reconstruction, but also replace the historical samples in the G11. The tree-ring data used in this thesis was collected from the sampling sites marked by green triangles in Figure 3.3. The locations of the meteorological stations which data is used for reconstruction calibration is marked by red (Duved) and blue (Östersund) circles. In this thesis work, new tree-ring samples were collected from the sites Håckervalen-top (1), Furuberget1 (4), Furuberget2 (6) and Håckervalen (7). Samples from sites Jens Perstjärnen (2), Öster Helgtjärnen (3), 4 and Lilla-Rörtjärnen (5) were collected in earlier efforts. Sites Rätan (8), Kyrkås (9) and Sunne (10) refer to the historical samples collected by Schweingruber and his colleagues in the 1970s. Parts of the samples from sites 2, 3, 4, 5, 8, 9 and 10 were used in G11. The samples from sites 1, 3, 5 and 7 were used for the analysis in Paper I. The samples from sites 1-5 and 8-10 were used for the analysis in Paper II. The samples from sites 1-7 were used in the new central Scandinavia April-September mean temperature reconstruction in Paper III. Figure 3.4 shows the temporal distribution at each sampling site of the samples used in the new reconstruction.

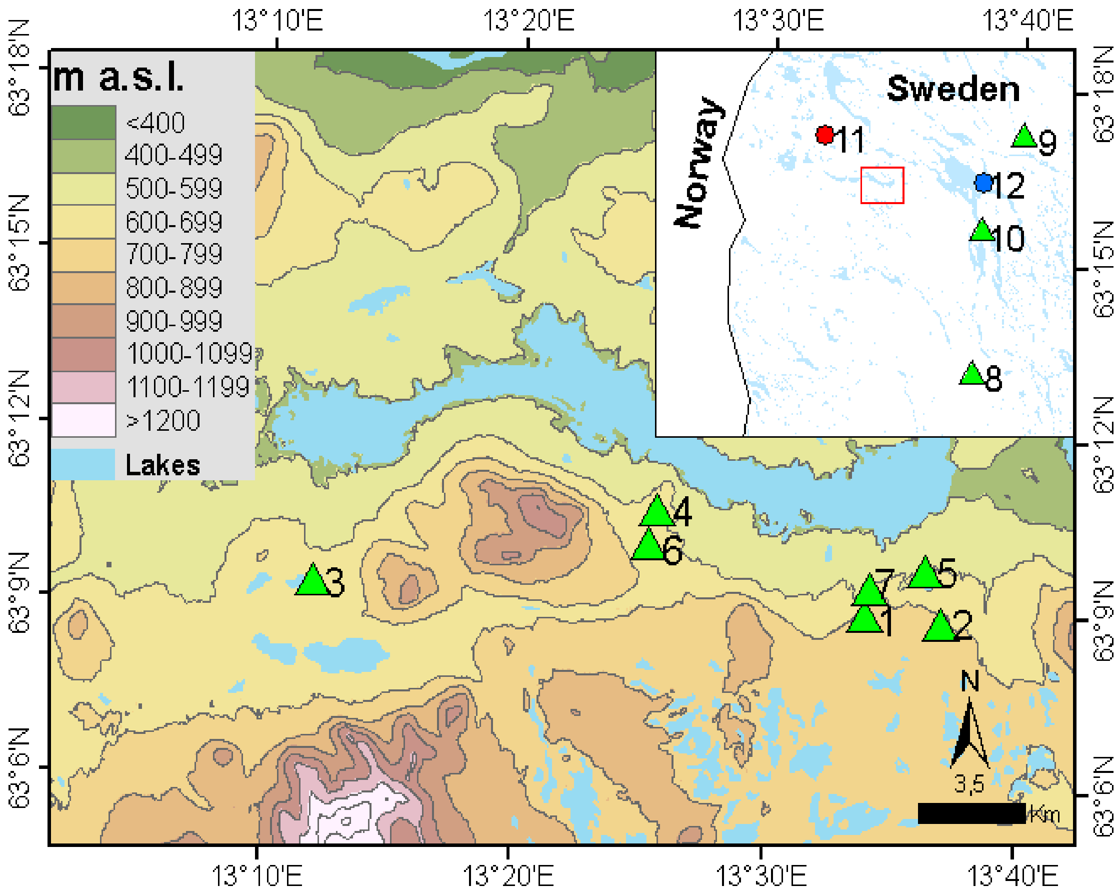

Figure 3.3 A map showing tree-ring sampling sites and the locations of the meteorological stations which data was used in this thesis work. Green triangles mark the locations of the tree-ring sampling sites, and circles mark the locations of Duved (red) and Östersund (blue) meteorological stations. Location: 1=Håckervalen-top; 2=Jens Perstjärnen; 3=Öster Helgtjärnen; 4=Furuberget1; 5=Lilla-Rörtjärnen; 6=Furuberget2; 7=Håckervalen; 8=Rätan; 9=Kyrkås; 10=Sunne; 11=Duved; 12=Östersund.

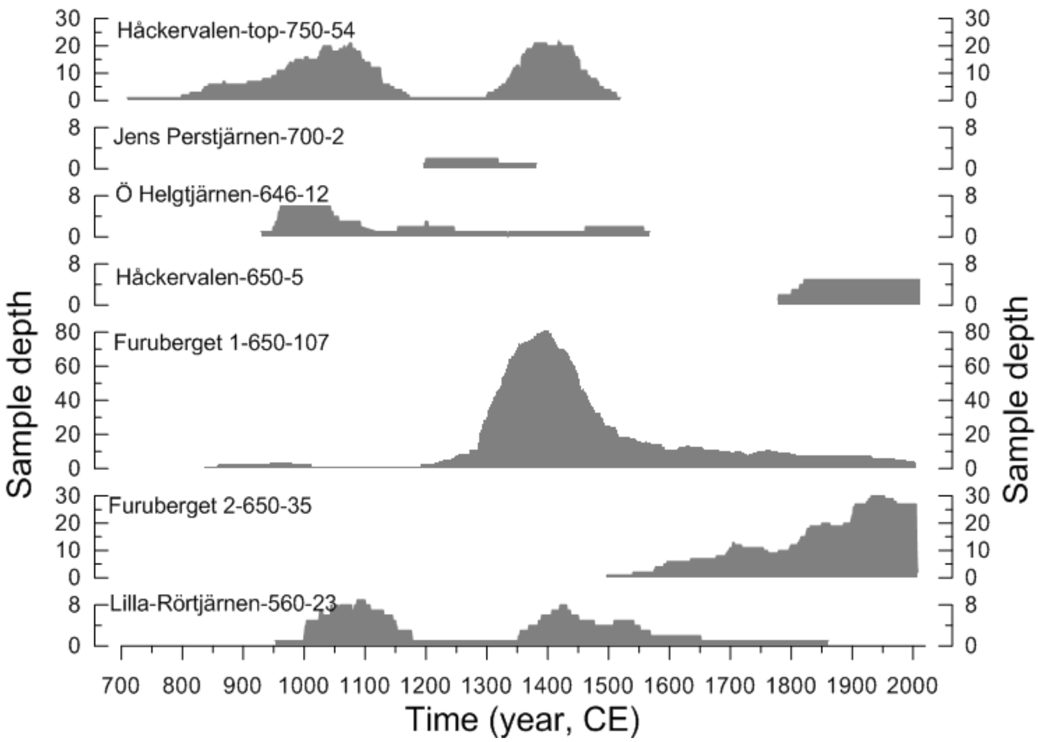

Figure 3.4 Sample replication and time span in each site. The site names, elevations and number of samples were given on the upper-left corner of each subplot.

Samples from living trees were also collected in order to update the reconstruction for the most recent period. Living tree samples were collected using an increment borer, while dead trees were sampled by cutting a disc using a chainsaw. Figure 3.5 shows a tree core extracted from a living Scots pine, and a disc cut from a dead tree lying on the ground.

(a) (b)

Figure 3.5 (a) A tree-ring sample extracted from a living Scots pine; (b) a disc cut from a dead tree.

3.5 Tree-ring width and density measurement

Back in the lab, the tree-ring samples were mounted on woody supporters, and then polished using sanding machines or sand papers to prepare a smooth surface for tree-ring width measurement. Tree-ring width (TRW) was measured using the Lintab 6 station (www.rinntech.de). The exact calendar year of each ring of each individual TRW series were dated by comparing the growth pattern with a dated Jämtland chronology (Gunnarson et al., 2003) using the software of TSAP (www.rinntech.de). Panel (a) in Figure 3.6 shows a cross section of a living tree sample where the wood cells can be clearly seen. The sharp boundary on the left side of each dark band (the latewood which is formed at the end of the growing season, and consists of small and thick-walled xylem cells) is a mark indicating the end of a growing season. The brighter part of the wood is called earlywood which formed at the start of the growing season with large and thin-walled xylem cells. Tree-ring width is the distance between a sharp boundary and the other one next it. MXD is the maximum density of a latewood. Latewood usually has higher density than earlywood.

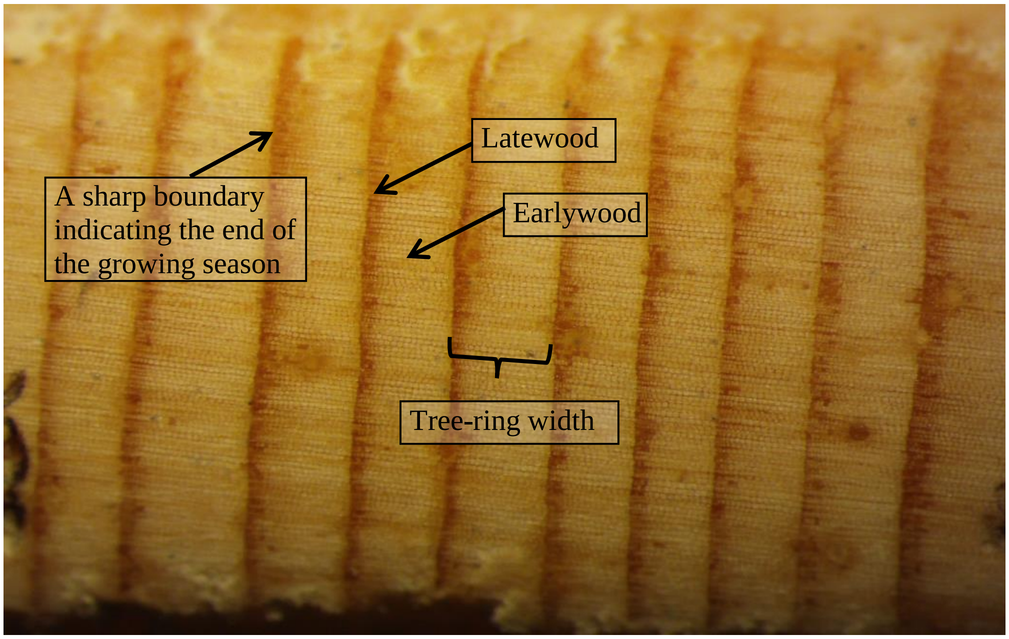

(a)

(b) (c)

Figure 3.6 Cross sections from (a) a living Scots pine, (b) a dry and (c) a waterlogged dead Scots pine sample.

The tree-ring samples were prepared for MXD measurements according to the techniques described in Schweingruber et al. (1978). A thin lath (1.20 mm in thickness) was cut from each of the samples using a twin-bladed circular saw, and was soaked in pure alcohol in a Soxhlet for at least 24 hours to remove extractives such as resin. The laths (air dried to 12% water content) were then mounted on a sample frame, and X-rayed with a narrow, high energy beam in the ITRAX multiscanner from Cox Analytical Systems (www.coxsys.se). The settings of ITRAX were set according to Gunnarson et al. (2011). The chrome tube in ITRAX was tuned to 30kV and 50mA, with 75ms steptime. The opening time of a sensor slit was set as 20µm at each step. After X-rayed, a 16-bit, greyscale, digital image with a resolution of 1270 dpi was produced for each sample, and its grey level was calibrated using a calibration wedge from Walesch Electronic. The MXD data was obtained from the images using WinDENDRO tree-ring image processing software (Guay et al., 1992). Figure 3.7 shows the main equipment for the MXD measurement (panel (a), (c), (d), (e)). Panel (b) shows the laths cut from tree-ring samples. Panel (f) shows a 16-bit digital image produced by ITRAX, which is ready for measuring the density value of each ring. The green lines were marked manually to define the boundaries of the latewood between which the density value was subsequently measured.

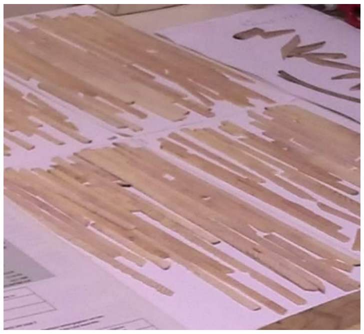

(a) (b)

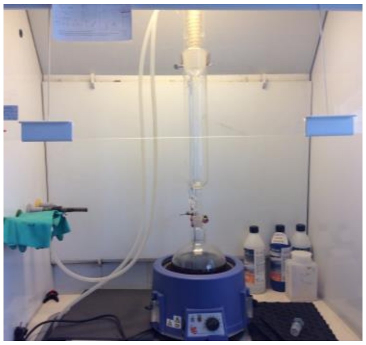

(c) (d)

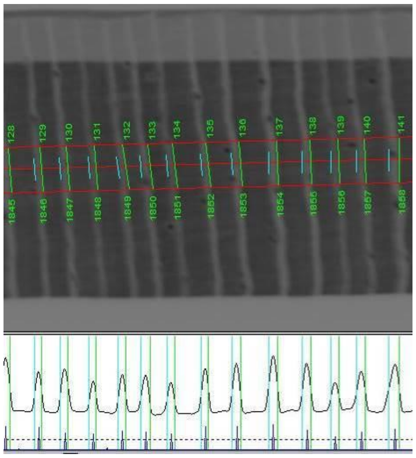

(e) (f)

Figure 3.7 (a) The saw used for preparing laths for the MXD measurement; (b) laths cut from tree-ring samples; (c) the soxhlet for removing extractives such as resin; (d) the frame used to fix the wood laths; (e) the ITRAX multiscanner for tree-ring MXD measurement; (f) a 16-bit digital image produced by ITRAX.

3.6 Standardisation and reconstruction

In this thesis work, RSFi, (Björklund et al., 2013) was used to remove the non-climatic signals from the tree-ring MXD series. After standardisation, the tree-ring MXD indices were produced. Then the indices were averaged to build a tree-ring MXD chronology. The individual signal-free curves and the signal-free regional curve were produced using the software ARSTAN (Cook, 1985).

The chronology was calibrated against the observed warm-season temperature from Duved meteorological station for the period 1890-2011. The established relationship from the calibration was then used to reconstruct the warm-season temperature for the past 1200 years.

3.7 Meteorological data from instrumental observations and model simulations

In this thesis work, observational temperature data was used to examine the climate signal in the TRW and MXD chronologies, and then was used for the temperature calibration to reconstruct past temperature variability (Paper I and III). Observational temperature data was also used to investigate the relationship between annual and summer temperature variability in central Scandinavia at different timescales (Paper IV). Simulated temperature were collected from climate models under Coupled Model Intercomparison Project Phase 5 (CMIP5, Taylor et al., 2012).

3.7.1 Observational temperature

Monthly temperature data from Duved (400 m a.s.l., 63.38˚N, 12.93˚E, the location is shown in Figure 3.3) meteorological station, was used to assess the temperature signal in the MXD chronology (Paper III). Since the data from this station only cover the period 1911-1979, we extended the data back to 1890 and up to 2011 by using linear regression on monthly temperature data from an adjacent station: Östersund (376 m a.s.l., 63.20˚N, 14.49˚E, the location is shown in Figure 3.3). A linear regression was done to relate the mean temperature of each 170 month from Östersund station to the one from Duved station. Data from Östersund explain on average 91.5% of the interannual variability in Duved monthly temperature (based on the overlapping period 1911-1979). The temperature data from Östersund came from two sources: the Nordklim data base (1890-2001) (Tuomenvirta et al., 2001), and Swedish Meteorological and Hydrological Institute (SMHI, 2001-2011).

Observational temperature data from one grid (the red dot shown in Figure 3.8) from the CRU TS3.22 2.5˚longitude × 2.5˚latitude grid dataset (Harris et al., 2014) was used to investigate the relationship between annual and summer temperature variability in central Scandinavia (Paper IV). The CRU gridded temperature was chosen instead of meteorological station data, because the gridded data is interpolated data which has similar resolution as the data from model simulations. The similar resolution enables the comparison between model and the observational data. The CRU gridded temperature was collected from the closest grid to the tree-ring sampling sites. The locations of the CRU and modeled grid are shown in Figure 3.8. The green star marks the location of the tree-ring sampling sites.

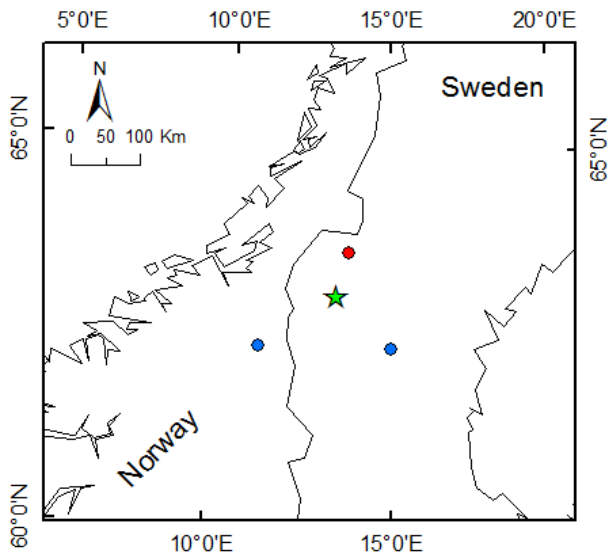

Figure 3.8 A map showing the closest grid (the red dot) to the tree-ring sampling sites from CRU TS3.22 2.5˚longitude ×2.5˚latitude dataset and two grids of HadCM3 historical simulation dataset (blue dots) used in Paper IV. The green star marks the location of the tree-ring sampling site.

3.7.2 Climate model data

The modeled temperature data used in Paper IV was collected from the two grids (blue dots shown in Figure 3.8) from the historical simulation (1860-2005 CE) performed by a coupled atmosphere-ocean general circulation model (AOGCM), HadCM3 (from the Met Office Hadley Centre, UK), which is one of the CMIP5 simulations. The CMIP5 is a framework that coordinates latest climate model simulation experiments for the climate change assessment, climate model diagnosis, validation, intercomparison and publication of model output data (Taylor et al., 2012). Under this framework, scientists are able to analyze AOGCMs in a systematic fashion, which serves to facilitate model improvement (Taylor et al., 2012). Historical simulations are the ones that simulate the 20th century climate using all forcings recommended by the CMIP5 project. HadCM3 model was used because it has the best performance on reproducing multi-century to millennium scale summer temperature variability in central Scandinavia comparing to other 10 CMIP5 last millennium simulations (not shown).

The modeled temperature data used for comparing to the new central Scandinavia warm-season temperature reconstruction is collected from 11 last millennium simulations performed by 11 CMIP5 climate models (data based on 10 simulations during 851-999)). Data were collected from mainly one grid and twice from four grids from the area of 12˚E-15˚E and 62˚N-64˚N. The tree-ring sampling sites are also inside this area. The number of sampling grids depends on the resolution of the atmosphere of the model. Detailed information about the models and the number of sampling grids is listed in Table 3.1.

Table 3.1 Information of the 11 CMIP5 global climate models. The resolution of the atmosphere of the model expressed by the number of longitudinal grids × the number of latitudinal grids. Number of grids indicates how many grids were chosen as sampling grid in each model.

Model	Institute/Country	Atmosphere resolution	Number of sampling grids
BCC-CSM1.1	BCC/China	128×64	1
CCSM4	NCAR/USA	288×192	4
CSIRO-Mk3L-1-2	UNSW/Australia	64×56	1
FGOALS-gl	LASG-IAP/China	72×45	1
FGOALS-s2	LASG-IAP/China	128×108	1
GISS-E2-R	NASA GISS/USA	144×90	1
HadCM3	MOHC/UK	96×73	1
IPSL-CM5A-LR	IPSL/France	96×95	1
MIROC-ESM	MIROC/Japan	128×64	1
MPI-ESM-P	MPI-M/Germany	196×98	1
MRI-CGCM3	MRI/Japan	320×160	4

4. Summary of papers

4.1 Paper I

In the central Scandinavian Mountains, summer temperature was reconstructed using TRW data for the past 3600 years (Linderholm and Gunnarson, 2005). That reconstruction was based on Scots pine tree-ring samples collected from living trees, dead trees lying on the ground and dead trees from lakes, where the trees originally grew on the shores of the lakes. Two recent studies have shown differences in the climatic response of Scots Pine growing in dry and lake-shore environments (Düthorn et al., 2013; Helama et al., 2013). Therefore, one question is if any difference in the temperature signal derived from lake-shore and tree-line pines could be detected. If this would be the case, this may cause temperature biases in reconstructions mainly built from subfossil (lake shore) wood.

The hypothesis was that the pines growing at the tree line should be the most sensitive to summer temperatures, compared to the trees having grown adjacent to small lakes at a lower elevation, since stressed trees (by low temperature at the tree line in this case) are more sensitive to climate than unstressed ones (Travis et al., 1990). Thus, any divergence in the TRW pattern in the subfossil (wet) and the tree-line (dry) samples during a period would indicate a change in the climate sensitivity of tree growing at lake shores (i.e. the TRW pattern of lake shore pines lose some sensitivity on representing the variability of summer temperature). This allowed us to assess if tree-ring chronologies mainly based on lake-shore TRW data may contain a biased summer temperature signal. The results provide information on how to make an optimal sampling strategy for TRW based regional temperature reconstruction.

New Scots pine TRW data from dry samples collected from trees lying on the mountain side between 700 and 800 m a.s.l. (around 50-100 m above the present tree line) were compared with Scots pine TRW data from subfossil lake-shore trees at elevations between 500 and 700 m a.s.l. during two periods: 950-1160 and 1320-1500. Parts of the subfossil material had previously been included in the central Scandinavian Scots pine chronology (Gunnarson, 2008).

The results showed that in the early period, 950-1160, belonging to the MCA, the chronologies based on both dry and subfossil samples were significantly correlated during most of the time, and that they show consistent variability on both interannual and decadal timescales. In the latter period, 1320-1500, belonging to the transition to the LIA, there was less agreement between the chronologies as indicated by the visual discrepancy between the series and the running correlation. Compared to the early period, the growth conditions appear to have been more variable at the tree line, especially on decadal timescales. The interannual variability is also more pronounced during this period, which likely indicates a more variable summer climate.

Comparing the tree-line and the subfossil data with temperature and precipitation showed that for the tree-line pines, a significant temperature signal was only found in July and August. For the lake-shore samples, in addition to significant positive correlations with temperatures in June, July and August, TRW was also significantly and negatively correlated to precipitation in July and August.

Our results showed that the local tree line in the central Scandinavia Mountains during the MCA and early LIA was about 140 m higher than at present. During the MCA, inferred to be a warm and dry period, pines from both tree-line and lake-shore environments showed coherent growth patterns on both interannual and multidecadal timescales. During the early LIA, however, the two sites showed less coherency, and the subfossil pines show less variability than the tree-line pines. The results implicate that the lake-shore trees may lose some of their sensitivity to temperature during cooler and wetter periods, possibly due to the effect of increasing water levels in the lakes. Therefore, temperature reconstructions based predominantly on subfossil lake-shore TRW samples may need to be re-evaluated.

4.2 Paper II

Building a millennium long chronology for temperature reconstruction needs large amounts of tree-ring samples. These samples cannot always be found at the same elevation. In the central Scandinavian Mountains, many samples covering the period 800-1150 were collected from above the present tree line. In observations, the temperature decreases with increasing elevation due to the atmospheric lapse rate. This raises a question that if absolute MXD values, where MXD data from high latitudes and altitudes is an exceptionally good temperature proxy, are affected by the lapse rate (i.e. the mean MXD value of tree-ring samples from high elevations is smaller than that of tree-ring samples from low elevations during a certain period). If so, this could bias reconstructions that are based on MXD data from different elevations, especially if their temporal coverage is uneven.

This issue was addressed in Paper II, where the effect of elevation on a MXD based reconstruction was investigated, and the MXD was derived from the samples presented in paper I. The sample replication at different elevations was different as shown in Figure 3.3 in Paper II. The results showed that the mean MXD values from trees growing in dry environments decreased with increasing elevation during 900-1150 and 1300-1550. It was shown that the existence of this elevation dependent difference in absolute MXD values can bias the trend of a composite chronology if the distribution of the samples from different elevation does not overlap in time. An example of the bias was shown based on the MXD data from Håckervalen and Furuberget. The results show that although both chronologies of these two sites individually captured a cooling trend, the final chronology based on both sites, actually expressed a positive warming trend which contradicts our knowledge of the temperature evolution of the last millennium.

To overcome the elevation problem, we adjusted the means of all groups of samples to the same value based on their relationship during the common period 1300-1550. A constant was added to or subtracted from all samples from each site in order to harmonize the MXD mean values of the different sites. The results showed that the trend bias in the final chronology was overcome when using the mean-adjusted data. The mean-adjustment method was then used to adjust the MXD samples in Paper III.

4.3 Paper III

In this paper, we extended G11 back in time to cover the past 1200 years, and removed the historical samples and added new samples. The new tree-ring MXD chronology was compared to instrumental monthly mean temperature from Duved meterological station. As shown in Figure 4.1, during the period 1890-2011, the new chronology has a significant positive correlation (at $p<0.01$ level) with individual monthly mean temperatures from April to September, and the highest correlation was found with mean April-September temperature ($r=0.77$). Mean April-September temperature was subsequently reconstructed using the new MXD chronology, which explains approximately 59% of the variance in the instrumental data. This is an improvement from G11, which explained 51% of the observed April-September temperature variability. Figure 4.2 shows the good agreement between reconstructed and observed mean April-September temperature at interannual to multidecadal timescales.

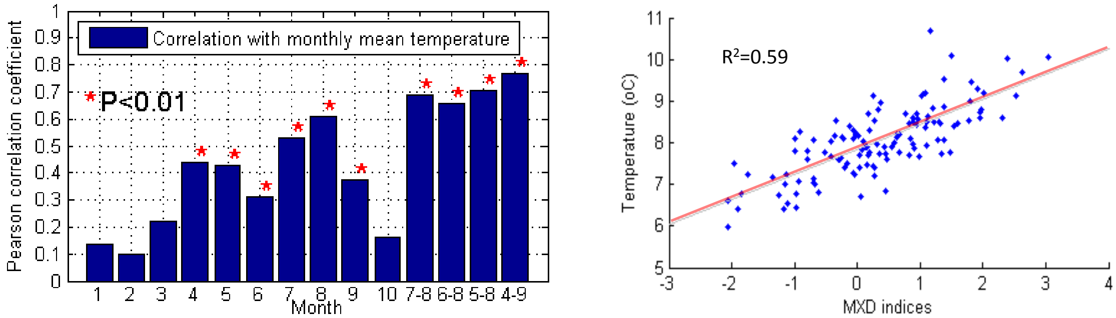

(a) (b)

Figure 4.1 (a) Correlation between the new tree-ring MXD chronology and monthly mean temperature over the period 1890-2011. Correlations are given from January to October of the growth year and July-August, Jun-August, May-August and April-September (warm season) average; (b) scatter plot of MXD data and the warm-season temperature.

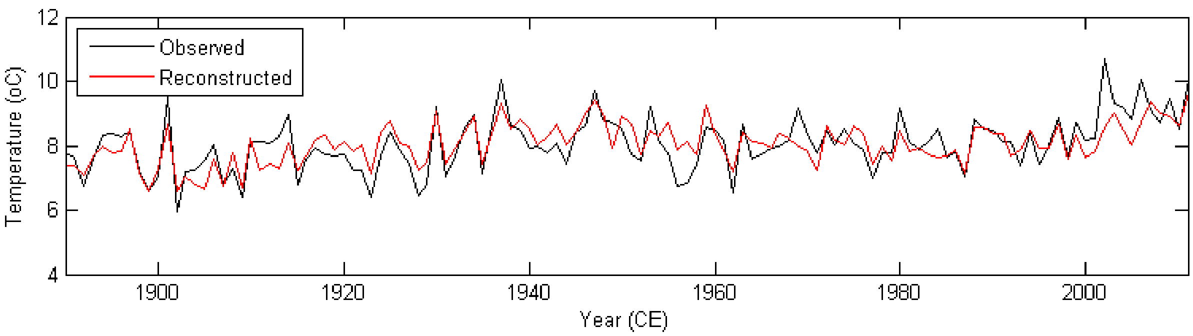

Figure 4.2 Comparison between reconstructed (red) and observed Duved (black) warm-season temperature for the period 1890-2011.

Table 4.1 shows the calibration and verification statistics. Clearly, the reconstruction passed all these statistic tests, indicating its validity.

Table 4.1 Calibration and verification statistics of the new reconstruction.

Tree-ring MXD based April-September temperature reconstruction			
Calibration period	1890-1950	1951-2011	1890-2011
Correlation, R	0.82***	0.67***	0.77***
Explained variance, R^2	0.67	0.46	0.59
No. of observations	61	61	122
Verification period	1951-2011	1890-1950	-
Explained variance, R^2	0.46	0.67	-
RE[#]	0.55	0.71	-
CE[#]	0.44	0.65	-

****the correlation is significant at p<0.01 significance level; [#]RE means reduction of error; CE means coefficient of efficiency.*

Warm-season temperature of the last 1200 years in central Scandinavia was reconstructed using the new MXD chronology. Figure 4.3 shows the spatial correlation between the reconstructed warm-season temperature and the gridded warm-season temperature from the CRU TS3.22 0.5˚ longitude × 0.5˚ latitude dataset during the period 1901-2011. The result shows that the new reconstruction represents the warm-season temperature variation with explained variance above 50% across much of central Scandinavia.

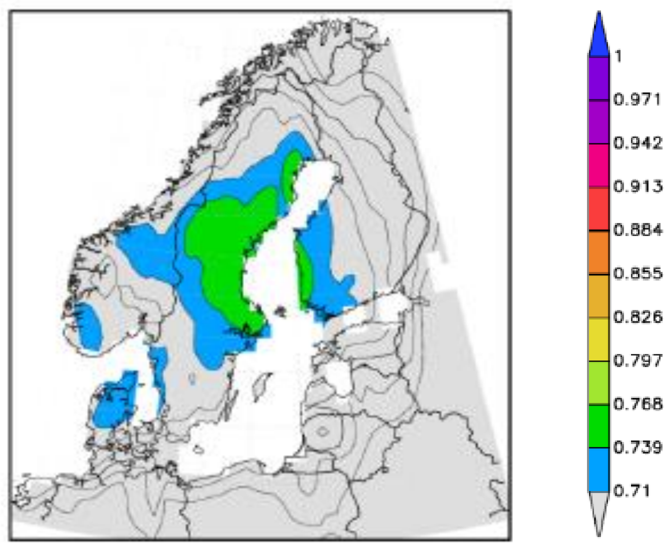

Figure 4.3 Spatial correlations of the reconstructed warm-season temperature from the new chronology in this study with the gridded warm-season temperature from CRU TS3.22 0.5˚longitude ×0.5˚latitude grid dataset during the period 1901–2011. Grey areas outside the r=0.71 isoline represent the correlations at $p < 0.001$ significance level. Color bars represent the magnitude of the correlations.

Figure 4.4 shows the importance of the application of the mean-adjusted data in the reconstruction. The reconstruction based on unadjusted data (blue curve) yields 0.4 ℃ lower average warm-season temperature during the period 850-1200 compared to the mean-adjusted reconstruction (grey/black curve).

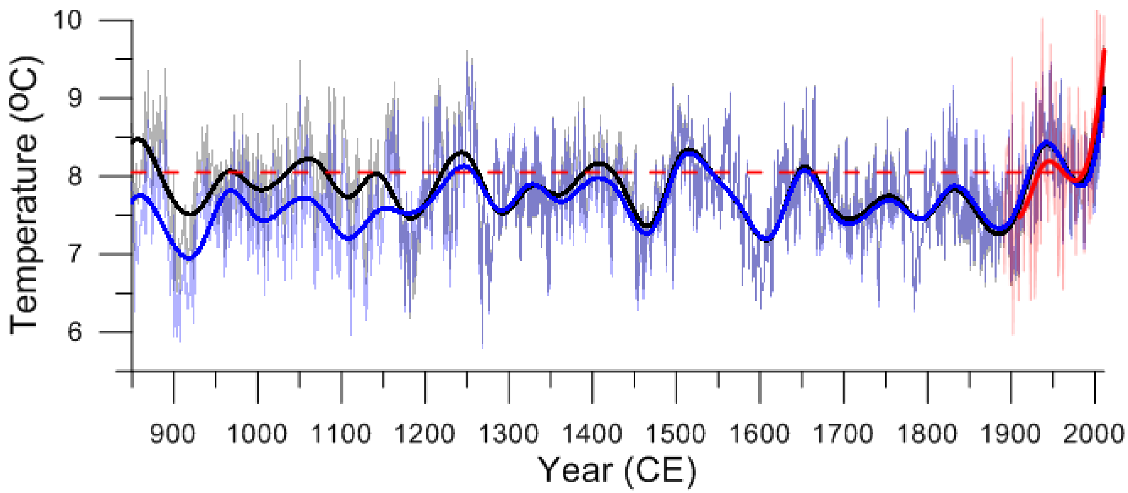

Figure 4.4 Comparison of the reconstructed warm-season temperature based on the mean-adjusted MXD samples (black) and the unadjusted MXD samples (blue). Red curves show the observed warm-season temperature variability extracted from Duved meteorological station. Light curves indicate the interannual variability, and the bold curves show the variability smoothed by 80-year spline filter. Dashed line shows the observed 1961-1990 mean warm-season temperature.

Figure 4.5 shows the reconstructed warm-season temperature variability in central Scandinavia, henceforth referred to as CSCAN. The main feature of CSCAN is a cooling trend between 850 CE and 1800 CE, followed by a sharp temperature increase after the mid-19th century. The late 17th century to early 19th century was the coldest long-term period during the past 1200 years, and the coldest 100 year appeared during the 19th century, and the coldest 10 and 30 year period appeared during the 17th century. The most recent 100 years is the warmest 100 years during the past 1200 years, which is consistent with the anthropogenic-induced global warming (IPCC, 2013). The warmest 10 and 30 year periods were found in the 13th century. Comparing the MCA with the current warming period, the warmest 100 year during the MCA was 0.1 ^{o}C cooler than the 20th century. The warmest 10 and 30 year periods during the 20th century were 0.2 and 0.1 ^{o}C cooler respectively than those during the 13th century.

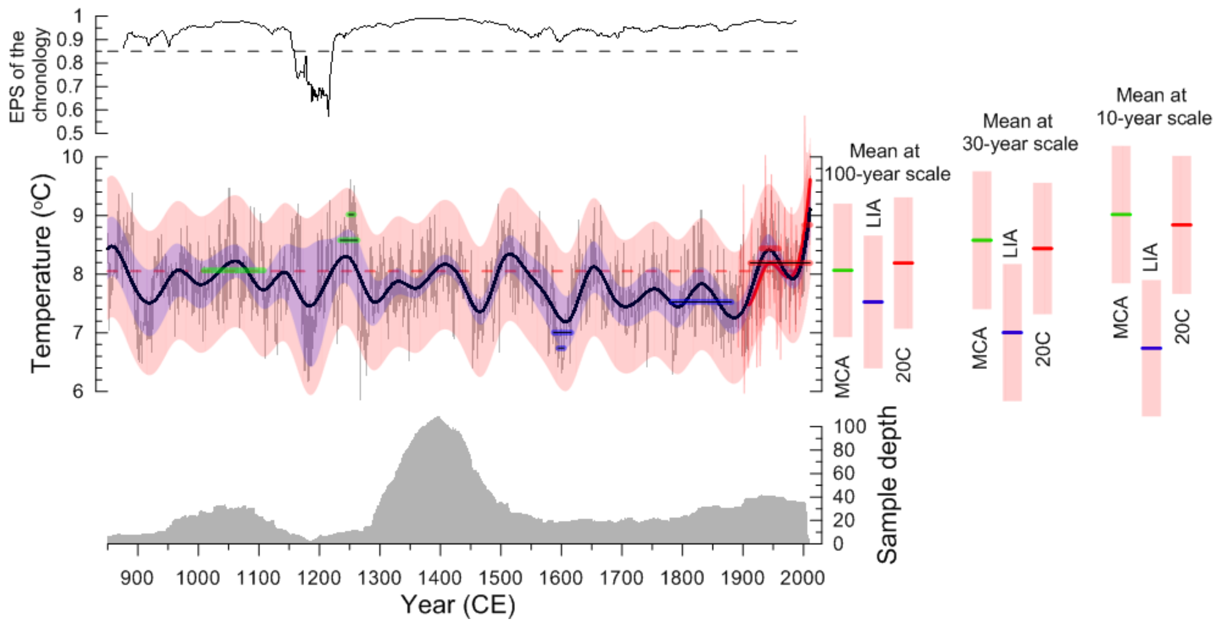

Figure 4.5 Annual (grey) and 80-year spline filtered (bold black) warm-season temperature variability over the period 850-2011 inferred from the new MXD chronology. Purple and pink shading indicate the chronology uncertainty and the total uncertainty of the reconstruction (including chronology uncertainty and reconstruction uncertainty). The grey shading and the thin black curve indicate the sample depth and EPS values (with the dashed line show the threshold of 0.85) of the chronology. Observed annual and 80-year spline filtered warm-season temperature is shown by the thin red curve and the bold curve, with the red dashed line indicating the 1961-1990 mean. The short lines in the right part of the figure mark the mean temperature levels of the warmest 100, 30 and 10 years in the MCA (green) and 20 century (red), and the coldest 100, 30 and 10 years in the LIA (blue). The time spans are marked on the corresponding positions on the temperature curve. The coloured short lines with thin solid black line in the center mark the time spans of the warmest and coldest 100, 30 and 10 years during the past 1200 years.

4.4 Paper IV

Is it suitable to use summer temperature sensitive proxies (i.e. tree-rings) to represent annual temperature conditions? This paper addressed this question by investigating the relationship between observed annual and summer temperature variability in our study area: central Scandinavia. As temperature varies on a variety of temporal scales, the relationship at different timescales was assessed based on temperature time series decomposed using the ensemble empirical mode decomposition (EEMD) method. The data were decomposed into five different frequency bands and a residual (C1-C6) representing the temperature variability at 2-4, 4-8, 8-16, 16-32, 32-64 and >64 year timescales using EEMD method.

Figure 4.6 shows the temporal evolution of the annual and summer temperature at the C1-C6 frequency bands during 1900 - 2005. The un-decomposed raw data shows that in general, summer temperatures have a slightly higher variance than annual ones. The variance of summer temperature has a much higher (93.0% of the total variance) power at the C1-C4 bands (2-32 year) than the annual temperature (59.1% of the total variance). On the longer timescales >32 year, however, the annual temperature show higher variability (40.9% of the total variance) than that of the summer temperature (7.0% of the total variance), which indicates that the long-term changes of the annual temperature are much more pronounced than those of the summer temperatures.

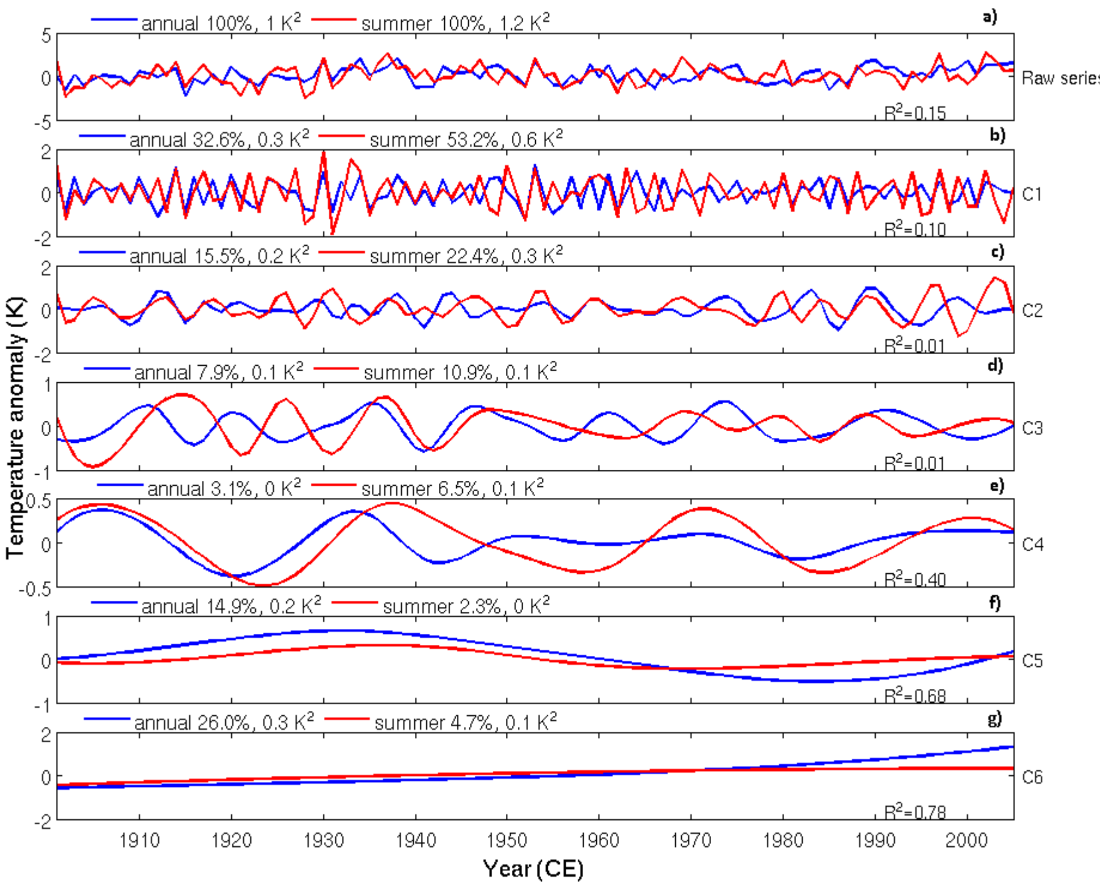

Figure 4.6 Comparison of the Annual (month 1-12, blue curves) and summer (month 6-8, red curves) observational grid temperature (anomalies relative to 1961-1990 means) at different timescales during 1901-2005: a) the original temperature, b) 2-4 year timescales, c) 4-8 year timescales, d) 8-16 year timescales, e) 16-32 year timescales, f) 32-64 year timescales, g) >64 year timescales. The correlation coefficient of each pair of temperatures is positive.

We evaluated one of CMIP5 climate models: the HadCM3 (Met Office Hadley Centre) on its performance on reproducing the scale dependent relationship between the annual and summer temperatures.

Figure 4.7 shows the correlation coefficients as a function of timescales for the observed (red) and simulated (blue) temperatures. Correlation between observed annual and summer temperature is significant (at $p<0.05$ significance level) at the 2-4 and >64 year timescales, while the correlation at 4-64 year timescales do not show a significant relationship. The simulated temperature shows higher correlation than the observed temperature at 4-16 year timescales and lower correlation at 2-4 and >16 year timescales.

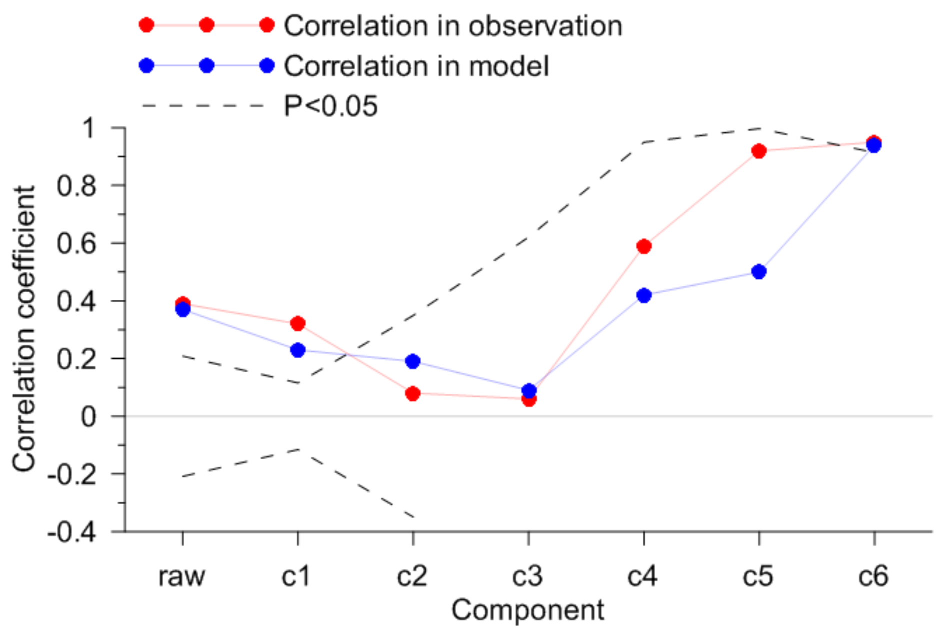

Figure 4.7 Correlation between the decomposed annual and summer observational (red circles) and simulated (blue circles) temperature series.

The results showed that the relationship between annual and summer temperature gets stronger as the timescales increase, except for the 4-16 year timescales at which it did not show any relationship. Summer temperature variability on short timescales (2-4 year) shows much higher variance than the annual variability, while annual temperature variability have a much higher variance at long timescales (>32 year) than summer. The results show that the summer temperature overall is not a reliable indicator of annual mean temperature variability. Although the high correlation exists at the 32-64 year timescales, the discrepancies in magnitudes and phases implicate an underestimation of the magnitude of the temperature variability and a mismatch of warm and cold peak between real and reconstructed temperature evolution. The HadCM3 historical simulation data showed serious variance bias in annual and summer temperature at 2-8 and >32 year timescales, especially for summer, compared to the observations. The model underestimated the strength of the relationships between the two temperatures at 2-4 year and >16 year timescales, while it overestimates the strength at timescales between 4 and 16 years, but overall the simulated relationship was similar to the observation. However, the model showed a weaker ability to reproduce the relationship at the 32-64 year timescales than those at other timescales.

5. A synthesis of the regional climate variability in the past 1200 years

5.1 Comparing CSCAN with other reconstructions

When comparing CSCAN to G11 (Fig. 5.1), CSCAN indicates lower temperature during the MCA and higher temperature during LIA than G11. The two reconstructions show coherent variability on multidecadal to century timescales during the period 1300-2000. Before 1300 CE, the two reconstructions are in less agreement especially during 1200-1250, which is the period when CSCAN has low EPS values due to low sample replication. However, despite having enough samples, G11 also shows low inter-series correlation during this period, which implicates a lack of a coherent signal among the series from the historical samples which were used in the previous reconstruction. Therefore, the variability indicated by CSCAN during 1200-1250 could be a signal reflecting the real temperature evolution.

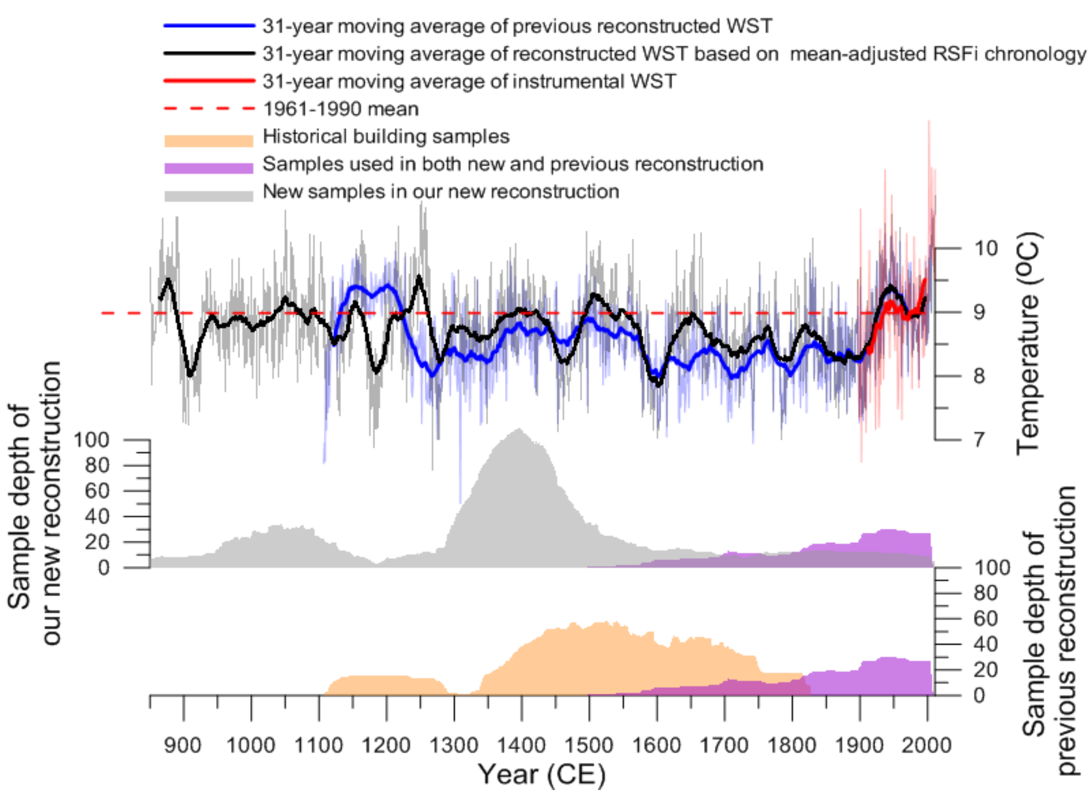

Figure 5.1 Comparison between CSCAN (thin grey curve) and G11 (thin blue curve). Bold black and blue curves show the variability after 31-year moving average filtering. The sample depths (number of trees) of the two reconstructions are marked by the grey and purple (CSCAN) and orange and purple (the previous reconstruction) shadings. The red curves indicate the observational temperature variability and its 31-year moving average. The dashed red curve marks the observed 1961-1990 mean temperature. WST=warm-season (April-September) temperature.

When comparing CSCAN with the most recently updated MXD reconstruction from northern Fennoscandia (as shown in Figure 5.2) (Matskovsky and Helama, 2014), the same feature is noted as in the comparison with G11: consistent variability at multidecadal and century timescales after 1300 CE, but less agreement before 1300 CE. It is clear that the low sample depth during the 13th century causes this offset, and hence, work on increasing the sample depth of the period before 1300 CE is still needed in central Scandinavia. However, it should be noted that the difference between central and northern Scandinavian temperatures may actually reflect a true difference in summer temperatures, which could be related to changes in the large-scale circulation affecting the region. Possibly changes in the spatial positions of the nodes of the NAO dipole over time (Ulbrich and Christoph, 1999; Zhang et al., 2008) could cause disruptions in the usually coherent summer temperature pattern. Since the instrumental record is too short, mechanism of the discrepancy needs to be investigated with assistance of the climate models which can simulate the climate state of the period before 1300 CE.

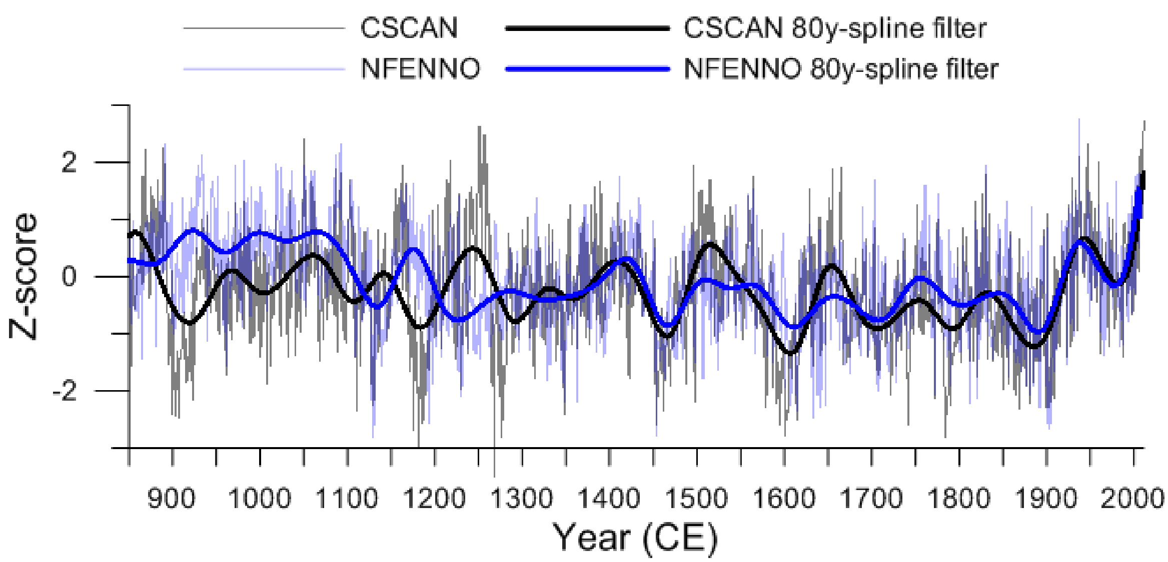

Figure 5.2 Comparison between CSCAN (black) with northern Fennoscandia (NFENNO) summer temperature reconstruction (blue) (Matskovsky and Helama, 2014). Bold curves show the variability after 80-year spline filtering. Z-scores were calculated based on 1890- 2006.

CSCAN was also compared to an extra-tropical northern hemisphere multi-proxy mean temperature reconstruction (Christiansen and Ljungqvist, 2012) in order to place it into a large spatial context. From Figure 5.3, we can see that both records support a general cooling trend during the last millennium, but the extra-tropical northern hemisphere mean temperature show a bigger cooling rate. This is mainly due to that the mean temperature reconstruction is partly based on low-temporal resolution paleo archives which have larger variance at millennium timescales

(Moberg et al., 2005). CSCAN suggests a warm peak around 1000-1100 during MCA, while the mean temperature reconstruction suggests the warm peak occur during 950 -1150. This could implicate that the warm maximum during MCA in central Scandinavia comes later than some other places in the extra-tropical northern hemisphere. Both the two reconstructions show a LIA around 1550-1900. The temperature recovery during the 16th century seems larger for the hemispheric scale mean temperature than that for CSCAN. The two reconstructions show quite coherent variability at multi-decadal to century timescales, especially during 1300-1600. This is similar with the results when CSCAN was compared with model data. This could implicate that during a 'peaceful' period such as MCA-LIA transition, the temperature evolution has a more coherent pattern at hemispheric scales which can be easily explained by natural external forcings, and easily simulated by physical functions such as those in climate models. However, during the periods such as MCA and LIA with strong climate anomalies, the temperature evolution at different regions starts to be divergent due to different speed of energy transport and feedback response which are definitely require more complex physical or chemical descriptions in climate models to be able to simulate the temperature evolutions.

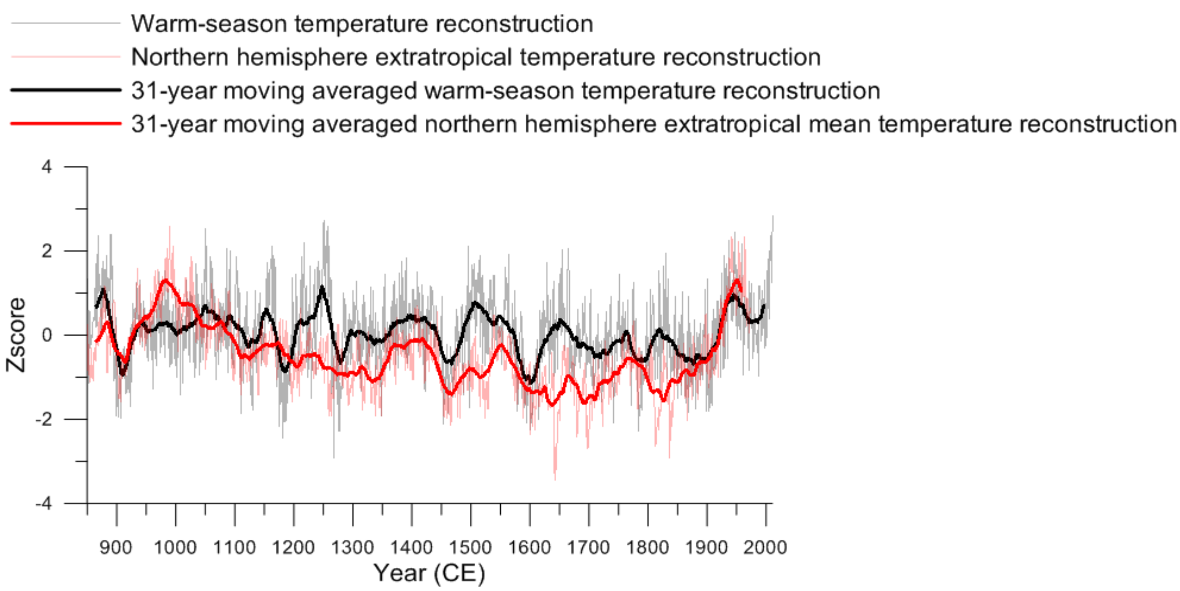

Figure 5.3 Comparison between CSCAN (thin grey curve) and the extra-tropical northern hemisphere multi-proxy mean temperature reconstruction (thin red curve) during 851-1973. Bold black and red curves show the variability after 31-year moving average filtering. Z-scores were calculated based on 1850-1973.

However, a comparison between CSCAN and the climate model ensemble mean (based on the data from 11 last millennium simulations performed by 11 CMIP5 climate models (data based on 10 simulations during 851-999)) of the warm-season temperature in central Scandinavia (Figure 5.4) also shows discrepancy during 1200-1250, where model data indicate a cooling trend, while proxy data show an intensive warming trend. Both model and proxy data show an overall cooling trend between 850 CE and 1300 CE, but they show a big discrepancy at multidecadal timescales during this time period. If we attributed discrepancy at the late 12^{th} century and the middle 13^{th} century to the uncertainty of the CSCAN due to its low samples replication during the two periods, however, it still cannot be explained why the model does not capture the multidecadal cooling at late 9^{th} century and early 12^{th} century and the warming at early 11^{th} century. The model seems to well capture the reconstruction between 1300 CE and 1700 CE, however, some periods such as late 14^{th} century and 17^{th} century, early 15^{th} century and early 16^{th} century, the model indicate small warm peaks. The cooling at around 1600 CE in the model does not as significant as the reconstruction. Between 1700 CE and 1850 CE, model and proxy show anti-phase temperature evolution. However, at this time period, most of Scandinavia warm-season/summer reconstructions show a good agreement on the variability at multidecadal timescales, which could implicate a bad performance of the model ensemble, mean on simulating the temperature variability at multidecadal timescales during late LIA. In general, the climate model ensemble mean can well simulate the multicentury scale warm-season temperature evolution at central Scandinavia during the last millennium. However, at multidecadal to century scales, the model exhibit better performance on capturing the temperature variability at the transition of MCA to LIA than the late MCA and late LIA.

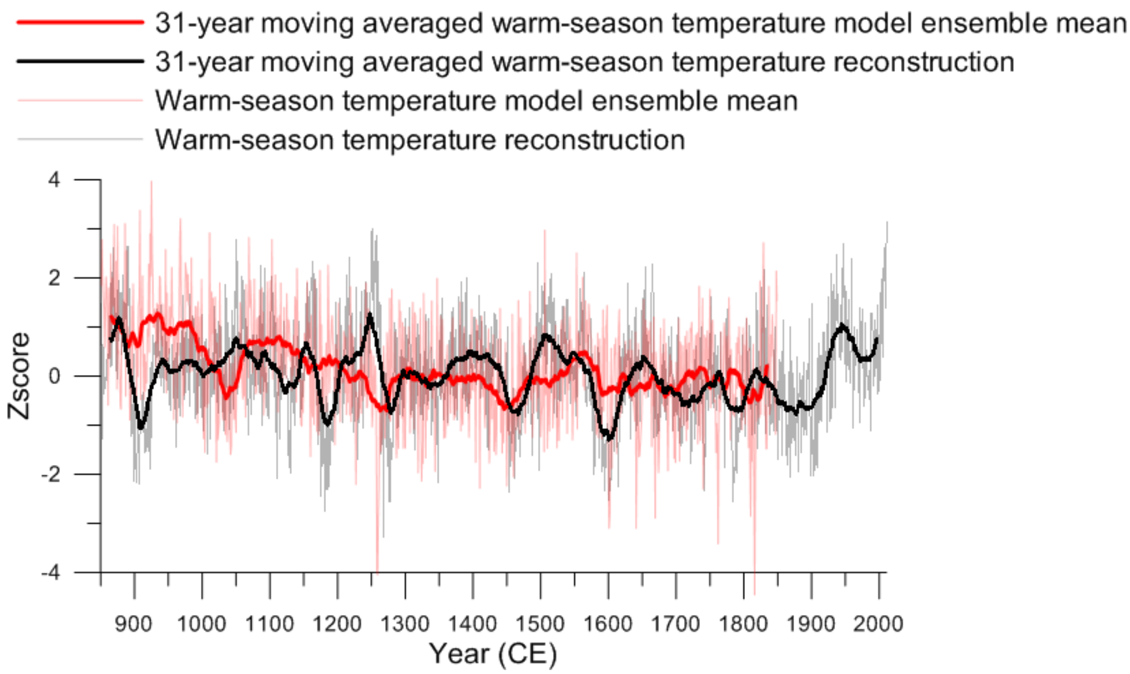

Figure 5.4 Comparison between CSCAN (thin grey curve) and the model ensemble mean warm-season temperature variability (thin red curve) at central Scandinavia during 851-1849. Bold black and red curves show the variability after 31-year moving average filtering. Model data during 851-999 (during 1000-1849) were extracted from surface (2m) air temperature dataset from 10 (11) last millennium simulations performed by 10 (11) CMIP5 climate models. Z-scores were calculated based on 1000-1849.

5.2 CSCAN and climate forcing

The main external climate forcings during the last millennium are solar variability and volcanic eruptions (Crowley, 2000). From Figure 5.5, it can be seen that there is no consistent relationship between the total solar irradiance (TSI, data from Steinhilber et al., 2012) and the evolution of CSCAN, although some of the periods with known drops in sunspot numbers (Stuiver and Quay, 1980) correspond to cool temperatures such as middle 15th century, late 13th century and 17th century. However, the cooling events all exhibit lags from years to decades. We should also notice that these periods also correspond to volcanic eruption events. In some periods such as early 17th century and late 19th century, although the solar irradiance keeps at high levels, the cooling events still occur. Shindell et al. (2003) indicate that regional-scale winter and annual mean temperature show significant response to solar forcing at decadal scales. Esper et al. (2012) found that the evolution of northern Scandinavia summer temperature follows the trend of solar forcing at millennium scale. These findings clearly show the close relationship between solar forcing and temperature evolution. However, in recent studies, Schurer et al. (2014) concludes that solar forcing probably had a minor effect on northern hemisphere climate over the past 1000 years, while volcanic eruptions and changes in greenhouse gas concentrations seem to be the most important influence during this period.

The influence of major volcanic eruptions is clear, where especially large eruptions are followed by cold summers. This is in agreement with the findings of Linderholm et al. (2014b), who found that large volcanic eruptions can cause a cooling of up to four years after the event. Also, in general periods with increased number of eruptions correspond to cooling on multidecadal timescales, which has previously been noted in Fennoscandia (e.g. McCarroll et al., 2013) showing the importance of volcanism as a summer climate forcing in the millennium context.

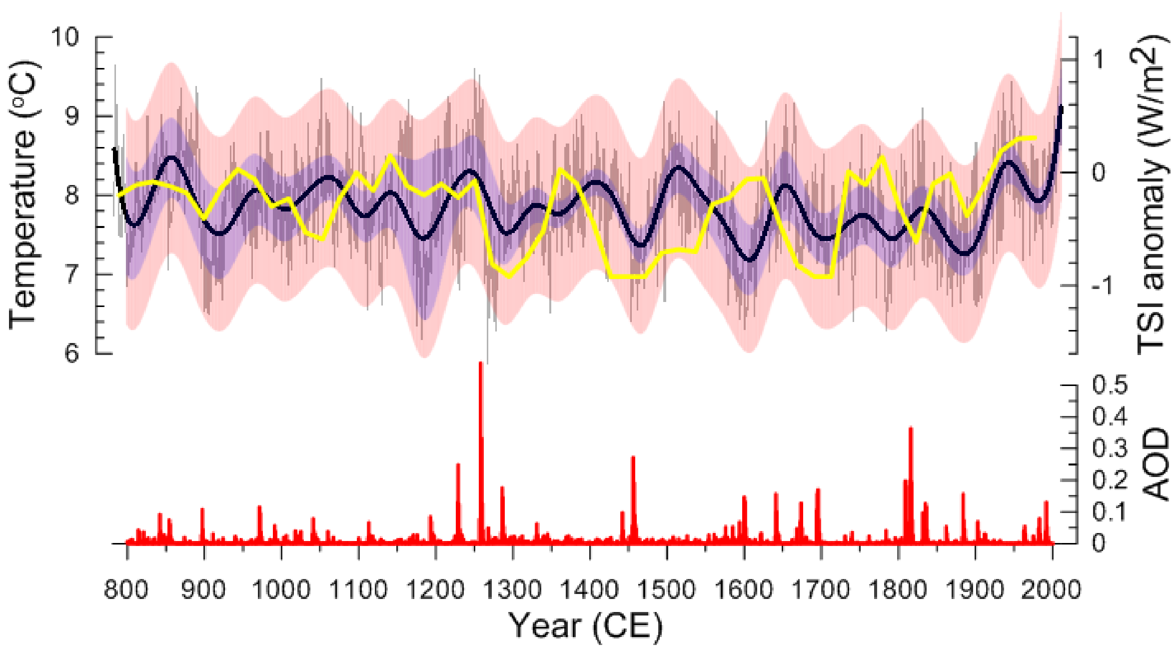

Figure 5.5 Annual (grey) and 80-year spline filtered (bold black) central Scandinavian warm-season temperature (April-September) variability over the period 783-2011 plotted against Total Solar Irradiance (TSI, yellow, based on ^{10}Be and ^{14}C from ice cores and tree rings) (Steinhilber et al., 2012) and yearly global average aerosol optical depth (AOD, red bars, based on ice core sulphate) (Crowley and Unterman, 2013). Purple and pink shading indicate the chronology uncertainty and the total uncertainty of the reconstruction (including chronology uncertainty and reconstruction uncertainty).

In addition to solar forcing and volcanic eruptions, the temperature variability is also strongly influenced by the atmospheric circulation such as NAO and oceanic circulation such as AMO. As mentioned above, NAO is the abbreviation of North Atlantic Oscillation, which represents a climatic phenomenon of fluctuations in the difference of atmospheric sea level pressure between the Icelandic low and the Azores high (Walker and Bliss, 1932). This index influences the strength and direction of westerly winds and storm tracks over the North Atlantic region, and thus influences the European climate (Rogers, 1997). The AMO represents the periodic variability of the main mode of SST in the North Atlantic Ocean, possibly linked to the thermohaline circulation (Kerr, 2000). The AMO is an important driver of the multidecadal variations of western European summer climate (Sutton and Hodson, 2005). The variability of NAO and AMO contains stochastic signals caused by climate system internal variability and trend signals caused by external forcings. A wavelet analysis (using the Matlab code developed by Torrence and Compo (1998)) was done on the temperature reconstruction and shows a persistent 2-8 year signal dominated during the whole course of the last 1200 years with enhanced power in the 11th, 13th, and 19-20th centuries (panel (d) in Figure 5.6). The 2-8 year signal in the North Atlantic region is usually related to the variability of the NAO (Cook et al., 2002). The strong signals during 11th, 13th and 19-20th century could imply the strong impacts of NAO during these periods. The period with strong 2-8 year signal in the temperature reconstruction coincides with the period with warm summer climate conditions. This implicates that during the warm period, the impacts of NAO on the warm-season temperature variability in central Scandinavia is more significant.

The temperature variability also shows strong 32-128 year signals during the early 10th century and the 11th-12th centuries. The signal at this timescale may be related to the AMO.

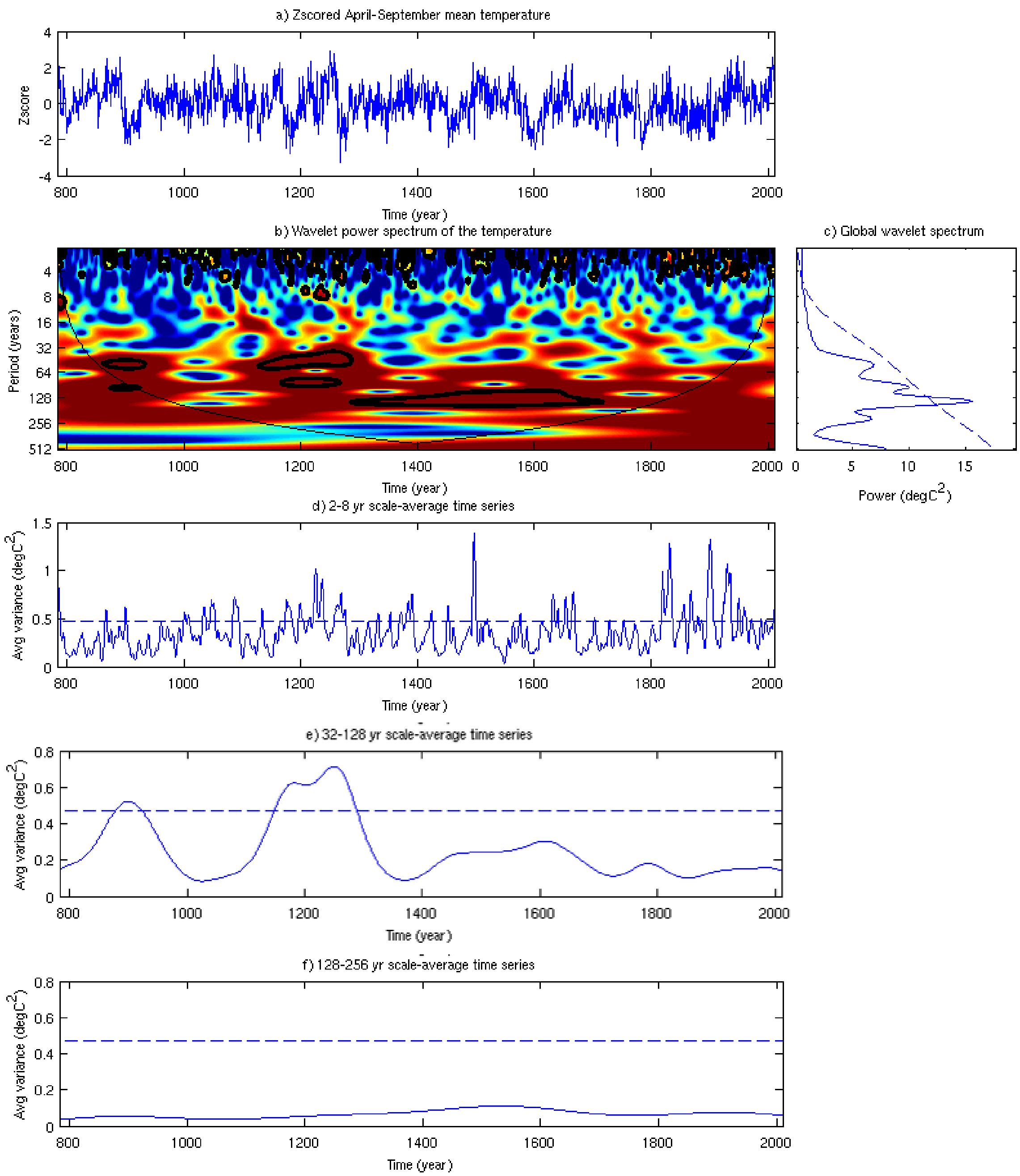

Figure 5.6 Wavelet analysis on CSCAN. The series in (a) is CSCAN series. The thick contours in panel (b) enclose regions of greater than 95% confidence level. The regions below the thin black curves in panel (b) indicate the 'cone of influence', where edge effects become important. Panel (c) shows the global power spectrum where the dashed curve indicates the 95% confidence level. Scale-averaged wavelet power over the 2-8 year band, 32-128 year band and 128-256 year band are shown in panel (d), (e) and (f), where dashed lines indicate 95% confidence level.

5.3 A synthesis of the summer climate variability

To gain better understanding of regional climate variability of the last millennium in central Scandinavia, the variability of other climate variables than temperature such as precipitation, sunshine hours should also be investigated. Unfortunately, there are very few high resolution datasets focusing on summer season from this region. One such dataset which has been developed recently is the central Scandinavia summer sunshine hour reconstruction based on stable carbon isotopes ($\delta^{13}C$) from tree rings (Salo et al., 2014). Here, the evolution of the CSCAN is compared with the sunshine reconstruction as well as a low-resolution humidity fluctuation reconstruction (Gunnarson et al., 2003) and an annual-resolution standardised precipitation-evapotranspiration index (SPEI) 0.5˚latitude ×0.5˚longitude grid reconstruction (Seftigen et al., 2014). The humidity fluctuation reconstruction is from a work to infer the Holocene humidity fluctuation in Sweden based on dendrochronological (the temporal distribution of subfossil wood samples from lakes) and peat stratigraphy data from the central Scandinavia. The SPEI is a drought index considering the effects of temperature and potential evapotranspiration. The SPEI grid dataset was developed over the whole Fennoscandia based on both tree-ring width and MXD data. The SPEI data for the comparison was extracted from the closest grid (63.10˚N, 13.5˚E) to the tree-ring sampling site in this study.

As shown in Figure 5.7, possible wetter periods were inferred in 1100-1250 and 1550-1700, and dryer periods in 1350-1550 according to Gunnarson et al. (2003). However, according to Seftigen et al. (2014), there are generally wet during these three periods. During 1000-1250 (corresponding to the late MCA) summers in central Scandinavia were dominated by warm and cloudy condition, but dominated by cold and sunny condition during 1650-1800 (corresponding to the LIA). During the 20th century, central Scandinavia was dominated by warm and cloudy condition. Temperature/sunshine relationship features correspond to those reconstructed for northern Fennoscandia (Gagen et al., 2011; Young et al., 2012; Loader et al., 2013). The proxy date suggests that only the early MCA (900-1000) is warm and sunny, while the latter part (1100-1250) was more cloudy and wet, suggesting an influence of warm and moist air masses in the region. A previous study suggested that the MCA was dominated by a persistent positive (1050-1450) winter NAO (Trouet et al., 2009), and possibly the associated increased winter precipitation contributed to the overall wet conditions during this period. The first century of the LIA (1450-1550) seems to have been quite variable in terms of temperature and sunshine. However, the humidity variability from the two datasets shows divergence where SPEI shows a wet condition, while the other inference shows a dry condition. This divergence could be due to the differences of the spatial representativeness between the two dataset, where SPEI represents a local area in central

Scandinavia, and the other inference represents the whole Sweden. Since precipitation feature can be very local, both of the two datasets could thus reflect a true past climate conditions. After 1550 CE, temperature became lower while summers were sunny, indicating an influence of cold arctic air masses during this period. This makes the inferred increased wetness between 1550 CE and 1700 CE difficult to explain. Possibly it could be attributed to enhanced winter precipitation, together with weaker evaporation in summer caused by low temperatures. However, Luterbacher et al. (2001) have shown that the period 1550-1700 was dominated by negative winter NAO conditions, which implies low winter precipitation. However, the winter NAO reconstruction by Cook et al. (2002) showed that the winter NAO was predominantly in its positive phase during 1550-1650, before going into a negative phase during 1650-1700. Further studies are needed to describe climate and its driving mechanisms during this period.

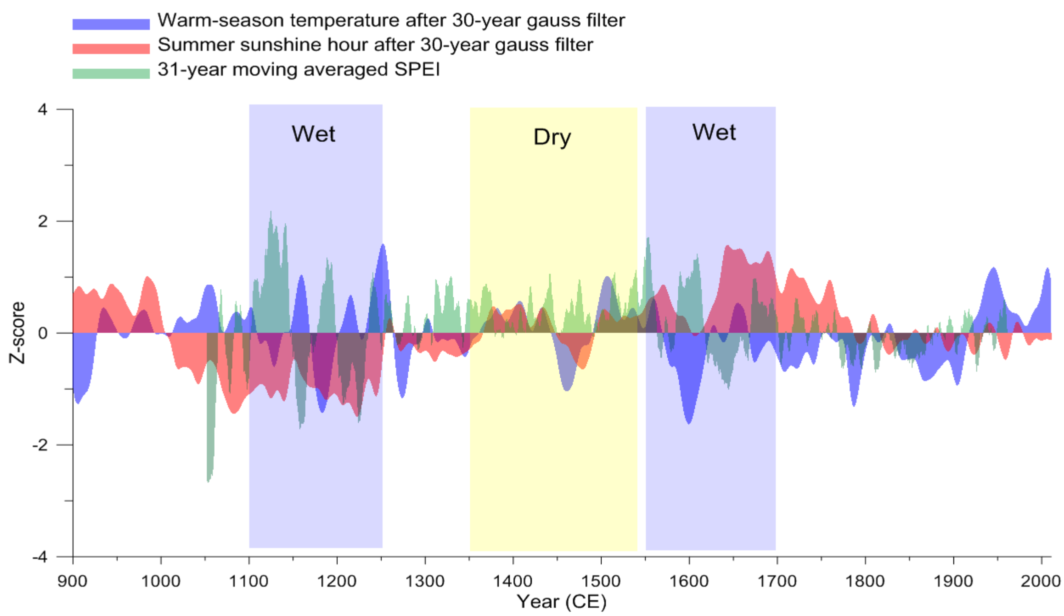

Figure 5.7 Warm season (April-September) temperature (blue, from CSCAN), summer sunshine hour (red, Salo et al., 2014) and SPEI (green, Seftigen et al., 2014) reconstructions. Shaded curves indicate the variability after 30-year low pass gauss filter for temperature and sunshine and after 31-year moving average filter for SPEI. Light blue and yellow background separately indicates the wetter and dryer periods inferred by Gunnarson et al. (2003).

5.4 Remaining challenges and future outlooks

One aim of this thesis work was to further our understanding of the climate variability in central Scandinavia. The temperature reconstruction has been extended back to the past 1200 years with the newly collected tree-line samples, now encompassing the MCA, which is a major step forward due to the general lack high-resolution, high-quality records covering this period. Also, the inclusion of new samples, all collected within a rather small area, and removal of the historical samples with an uncertain origin and climate sensitivity made the new reconstruction more reliable. However, some periods, such as that around late 12th century, still have too few samples, and the EPS value during that period is still below 0.85. Thus, one of the remaining challenges is to find samples in this region to increase the sample replication in this period. Efforts should be also made to extend the tree-ring MXD based temperature reconstruction further back in time. The final aim is to build a multi-millennia long tree-ring MXD chronology and reconstruct the warm-season temperature back to past millennia in this region. This work will benefit our understanding of the past temperature variability back to thousands of years at interannual to multicentury scales, and will complement the climate information inferred from other low-resolution paleoclimate proxies such as lake sediments, speleothem, peat stratigraphy and pollen. Future work should also focus on combining these proxies together by picking the signals from the dominant frequency which the proxies can reflect, such as the work done by Moberg et al. (2005).

In addition to temperature, other climate variables such as precipitation, humidity and sunshine hour are also important for our understanding natural climate changes in this region prior to the period with strong anthropogenic forcing. Efforts should also be made to investigate the interaction between these climate variables. Together with climate models, one important objective is to investigate and understand the mechanisms and processes behind the observed climate variability. This would help improving climate models to better simulate climate variability under natural conditions. The challenge is that there few hydroclimate reconstruction from this region and there is lack of the systematic model-data comparison metrics.

Climate changes in different seasons such as summer and winter are different in their magnitude and timing (regarding the warming rate), which has been detected using instrumental data. These differences likely apply also to the past under natural forcing conditions due to different feedback responses to natural external forcings in different seasons. The information of past climate changes in other seasons is also important for understanding the dynamics mechanism and processes of climate changes under natural forcing conditions. However, most of the paleoclimate reconstructions at interannual to century scales can only reflect the climate variability in summer. Still little is known of how the climate in other seasons varied in the past. One possible future effort could also be made to explore statistical or dynamical relationships of climate variability between summer and other seasons. In this thesis work, a pioneering study has been done for exploring the similarity between annual and summer temperature variability at different timescales in central Scandinavia. Future work could extend the study to other climate variables, and also extend the spatial scale.

6. Conclusions

1) The local tree line in central Scandinavia during the MCA and early LIA was about 140 m higher than the present one. During the MCA, pines from the tree line and lake-shore environments showed coherent growth patterns on both short- and long-term timescales, while during the early LIA, pines from both environments showed less coherency, and the subfossil pines from lake-shore environments showed less variability (interannual to decadal timescales) than the tree-line pines. This indicates that the lake-shore trees may lose some of their sensitivity to temperature during wetter periods, which implies that temperature reconstruction based predominantly on subfossil lake-shore trees may need to be re-evaluated.

2) Mean absolute MXD values varied notably with elevation in the central Scandinavian Mountains with higher elevation having lower MXD values due to the occurrence of the temperature gradients along altitudes. This difference was greater than the difference caused by low-frequency temperature variations (e.g. going from the MCA to the LIA). Without a continuous overlap in samples from different elevations, a chronology may be biased when the data is standardised. A mean-adjustment method aiming at adjusting the mean MXD values of the samples from each elevation was developed to overcome this problem. The reconstruction based on unadjusted data yielded 0.4 ℃ lower average warm-season temperature during the period 850-1200 compared to the mean-adjusted reconstruction.

3) A previous Jämtland tree-ring MXD chronology was updated and extended with newly collected tree-ring samples, and used to reconstruct warm-season temperature (April-September) in central Scandinavia for the period 850-2011. The new reconstruction suggests a MCA during ca. 1000-1100, followed by a transition period before the onset of the LIA proper in the mid-16th century. During the last 1200 years, the late 17th century to early 19th century was the coldest period in central Scandinavia, and the warmest 100 years occurred during the most recent century. The new reconstruction suggests lower temperature during late MCA and higher temperature during LIA than the previous reconstruction. The reconstruction shows regional differences in temperature evolution between northern and central Scandinavia before 1300 CE, which suggests overall colder climate conditions in central Scandinavia before 1200 CE, and warmer conditions during 1200-1300, and phase mismatches between the two temperature evolutions at multidecadal to century timescale. The serious mismatch during 1150-1250 is likely due to lack of samples in the central Scandinavia temperature reconstruction during this period.

4) During 1100-1250 (late MCA defined by the previous study), central Scandinavia is dominated by warm, cloudy and wet climate conditions, while during the LIA, this region was dominated by

cold and sunny summers and partly overall wet conditions. The transition period between the MCA and LIA (around 1350-1550 CE) was dominated by dry conditions. During this period, temperatures were positively correlated with sunshine hours at multidecadal to century timescales, which was different from MCA and LIA.

5) For central Scandinavia, the summer temperature overall is not a good 'proxy' for the annual temperature especially at the 2-16 year timescales. The model-proxy comparison suggests that HadCM3 has a good performance on reproducing the relationship, but show serious problems on reproducing variance of annual and summer temperature at different timescales, especially for summer and timescales longer than 32 years.

Acknowledgements

I wish to express my deepest sense of gratitude to my supervisors: Hans Linderholm, Deliang Chen and Björn Gunnarson. To Hans, thanks for introducing me to dendroclimatology, guiding me from knowing almost nothing about my PhD topic to getting a PhD degree. Thanks for your patient tutoring, support and encouragement. To Deliang, thanks for your patient guidance and invaluable advices. Without your trust, support and encouragement, I would never have been able to finish my PhD work. Thank you for generously sharing your knowledge and invaluable experiences both in life and research which really benefit me a lot. To Björne, thanks for sharing your knowledge on paleoclimate research and your guidance on data collection and processing. I really enjoy the time during my visits in the Dendrolab in Stockholm.

I would also like to thank Mauricio Fuentes, Jesper Björklund, Petter Stridbeck, Emad Farahat, Eva Rocha, Riikka Salo, Kristina Seftigen and her brother Peter, Daniel Yirgaw, Björn Gunnarson, Hans Linderholm, Paul Krusic, Ugyen Dorji for your great help and the fun time during the multi-fieldworks in Jämtland. Without your help, the research presented in this thesis would not have been possible. I would also like to thank Laura McGlynn and Håkan Grudd for assistance in the MXD measurements, and also thank Kristina, Prof. Dan Hammarlund and Prof. Heikki Seppä for sharing your paleoclimate data. Especially I would like to thank Jesper for sharing your knowledge, skills and ideas. You are such a nice and big guy who is always ready to help people. Thank Andrea for your great help at the last stage of my PhD thesis work!

A big thank to all lovely GULD members: Kristina, Jesper, Petter, Andrea, Mauricio, Emad, Riikka, Eva, Hans and Björne. I really enjoyed the time we spent together. With you guys, I feel like having a big family here in GVC, and you have been my constant source of support and encouragement. I will always treasure our friendship and all things we have experienced together.

I would also like to thank all the people at Department of Earth Sciences. You made me have such a nice time at GVC during my PhD study. Thank you for your inspiration and encouragement. Especially send my thanks to Yumei and Tinghai for your great help since I arrived in Sweden. Thanks to Alexander Walther for your help during my 'Institutionstjästgöring', and to Shiho and Sam for correcting my thesis. Many thanks to Anders Omstedt for your advice and encouragement. I would also like to thank all the fellow PhD students for your inspiration and encouragement. Best wishes to your research work!

Last but not least, I would like to thank my parents and my cousin for being a constant source of trust, support and encouragement. To my beloved wife - Xuefei Zhang, thank you for being supportive, understanding, sharing my happiness and sadness during my PhD study. I would never have been able to make it without you!

References

Adger, W. N., N. W. Arnell, and E. L. Tompkins (2005), Successful adaptation to climate change across scales. *Global environmental change*, 15(2), 77-86.

Baillie, M.G.L., and J.R. Pilcher (1973), A simple cross-dating program for tree-ring research. *Tree-Ring Bulletin*, 38, 35–43.

Björklund, J. A., B. E. Gunnarson, P. J. Krusic, H. Grudd, T. Josefsson, L. Östlund, and H. W. Linderholm (2013), Advances towards improved low-frequency tree-ring reconstructions, using an updated Pinus sylvestris L. MXD network from the Scandinavian Mountains, *Theoretical and applied climatology*, 113(3-4), 697-710.

Bojariu R, and F. Giorgi (2005), The North Atlantic Oscillation signal in a regional climate simulation for the European region, *Tellus A*, 57(4), 641-653.

Bradley, R. S. (1999), Paleoclimatology: reconstructing climates of the Quaternary, Academic Press.

Briffa, K. R., T. S. Bartholin, D. Eckstein, P. D. Jones, W. Karlén, F. H. Schweingruber, and P. Zetterberg (1990), A 1,400-year tree-ring record of summer temperatures in Fennoscandia. *Nature*, 346, 434-439.

Briffa, K. R., P. D. Jones, F. H. Schweingruber, W. Karlén, and S. G. Shiyatov (1996), Tree-ring variables as proxy-climate indicators: problems with low-frequency signals, in Climatic Variations and Forcing Mechanisms of the Last 2000 Years, edited, pp. 9-41, Springer.

Briffa, K. R., P. D. Jones, T. S. Bartholin, D. Eckstein, F. H. Schweingruber, W. Karlen, P. Zetterberg, and M. Eronen (1992), Fennoscandian summers from AD 500: temperature changes on short and long timescales, *Climate dynamics*, 7(3), 111-119.

Broecker, W. S. (2001), Paleoclimate: was the medieval warm period global?. *Science*, 291(5508), 1497-1499, doi: 10.1126/science.291.5508.1497.

Chen, D., and C. Hellström (1999), The influence of the North Atlantic Oscillation on the regional temperature variability in Sweden: spatial and temporal variations, *Tellus A*, 51(4), 505-516.

Christiansen, B., and F. C. Ljungqvist (2012), The extra-tropical Northern Hemisphere temperature in the last two millennia: reconstructions of low-frequency variability. *Climate of the Past*, 8(2), 765-786.

Cook, E. R. (1985), A time series analysis approach to tree ring standardization. Dissertation, University of Arizona.

Cook, E. R., and K. Peters (1981), The smoothing spline: a new approach to standardizing forest interior tree-ring width series for dendroclimatic studies. *Tree-ring bulletin*, 41, 45-53.

Cook, E. R., and L. A. Kairiukstis (Eds.) (1990), Methods of dendrochronology: applications in the environmental sciences. Springer Science & Business Media.

Cook, E. R., R. D. D'Arrigo, and M. E. Mann (2002), A well-verified, multiproxy reconstruction of the winter North Atlantic Oscillation Index since ad 1400*, *Journal of Climate*, 15(13), 1754-1764.

Cook, E. R., K. R. Briffa, D. M. Meko, D. A. Graybill, and G. Funkhouser (1995), The 'segment length curse' in long tree-ring chronology development for palaeoclimatic studies, *The Holocene*, 5(2), 229-237.

Crowley, T. J. (2000), Causes of climate change over the past 1000 years. *Science*, 289(5477), 270-277.

Crowley, T. J., and T. S. Lowery (2000), How warm was the medieval warm period?. *AMBIO: A Journal of the Human Environment*, 29(1), 51-54.

Crowley, T., and M. Unterman (2013), Technical details concerning development of a 1200-year proxy index for global volcanism, *Earth Syst. Sci. Data*, 5, 187-197.

D'Arrigo, R., R. Wilson, and G. Jacoby (2006), On the long-term context for late twentieth century warming, *Journal of Geophysical Research:* Atmospheres (1984–2012), 111(D3), doi: 10.1029/2005JD006352.

Düthorn, E., S. Holzkämper, M. Timonen, and J. Esper (2013), Influence of micro-site conditions on tree-ring climate signals and trends in central and northern Sweden, *Trees*, 27(5), 1395-1404.

Erlandsson, S. (1936), Dendrochronological studies. Stockholm's College Geochronological Institute Rep. 23, Uppsala, Sweden, 116 pp.

Esper, J., K. Treydte, H. Gärtner, and B. Neuwirth (2001), A tree ring reconstruction of climatic extreme years since 1427 AD for Western Central Asia. *The Palaeobot*, 50, 141-152.

Esper, J., E. R. Cook, and F. H. Schweingruber (2002), Low-frequency signals in long tree-ring chronologies for reconstructing past temperature variability, S*cience*, 295(5563), 2250-2253.

Esper, J., D. C. Frank, M. Timonen, E. Zorita, R. J. Wilson, J. Luterbacher, S. Holzkämper, N. Fischer, S. Wagner, and D. Nievergelt (2012), Orbital forcing of tree-ring data, *Nature Climate Change*, 2(12), 862-866.

Esper, J., U. Büntgen, M. Timonen, and D. Frank (2012), Variability and extremes of northern Scandinavian summer temperatures over the past two millennia. *Global and Planetary Change*, 88, 1-9.

Esper, J., E. Duethorn, P. J. Krusic, M. Timonen, and U. Buentgen (2014), Northern European summer temperature variations over the Common Era from integrated tree-ring density records. *Journal of Quaternary Science*, 29(5), 487-494.

Folland, C. K., J. Knight, H. W. Linderholm, D. Fereday, S. Ineson, and J. W. Hurrell (2009), The summer North Atlantic Oscillation: past, present, and future, *Journal of Climate*, 22(5), 1082-1103.

Fritts, H. C., J. E. Mosimann, and C. P. Bottorff (1969), A revised computer program for standardizing tree-ring series. *Tree-Ring Bulletin*, 29(1-2), 15-20.

Fritts, H. (1976), Tree rings and climate, edited, London, New York, San Francisco: Academic Press.

Gagen, M., E. Zorita, D. McCarroll, G. H. Young, H. Grudd, R. Jalkanen, N. J. Loader, I. Robertson, and A. Kirchhefer (2011), Cloud response to summer temperatures in Fennoscandia over the last thousand years, *Geophysical Research Letters*, 38(5), doi: 10.1029/2010GL046216.

Goosse H., H. Renssen, A. Timmermann, and R.S. Bradley (2005), Internal and forced climate variability during the last millennium: a model-data comparison using ensemble simulations. *Quat Sci Rev* 24:1345–1360.

Goosse, H., E. Crespin, S. Dubinkina, M. F. Loutre, M. E. Mann, H. Renssen, Y. Sallaz-Damaz, and D. Shindell (2012), The role of forcing and internal dynamics in explaining the "Medieval Climate Anomaly", *Climate dynamics*, 39(12), 2847-2866.

Gordon, G. A., B. M. Gray, and J. R. Pilcher (1982), Verification of dendroclimatic reconstructions, in Climate from tree rings, edited, Cambridge, Cambridge University Press, 58–61.

Grove, J. M. (2001), The initiation of the "Little Ice Age" in regions round the North Atlantic, in The Iceberg in the Mist: Northern Research in pursuit of a "Little Ice Age", edited, pp. 53-82, Springer.

Grove, J. M., and R. Switsur (1994), Glacial geological evidence for the Medieval Warm Period, *Climatic Change*, 26(2-3), 143-169.

Grudd, H., K. R. Briffa, W. Karlén, T. S. Bartholin, P. D. Jones, and B. Kromer (2002), A 7400-year tree-ring chronology in northern Swedish Lapland: natural climatic variability expressed on annual to millennial timescales. *The Holocene*, 12(6), 657-665.

Guay, R., R. Gagnon, and H. Morin (1992), A new automatic and interactive tree ring measurement system based on a line scan camera, *The Forestry Chronicle*, 68(1), 138-141.

Gunnarson, B. E. (2001), Lake level changes indicated by dendrochronology on subfossil pine, Jämtland, central Scandinavian Mountains, Sweden, *Arctic, Antarctic, and Alpine Research*, 274-281.

Gunnarson, B. E. (2008), Temporal distribution pattern of subfossil pines in central Sweden: perspective on Holocene humidity fluctuations, *The Holocene*, 18(4), 569-577.

Gunnarson, B. E., and H. W. Linderholm (2002), Low-frequency summer temperature variation in central Sweden since the tenth century inferred from tree rings, *The Holocene*, 12(6), 667-671.

Gunnarson, B. E., A. Borgmark, and S. Wastegård (2003), Holocene humidity fluctuations in Sweden inferred from dendrochronology and peat stratigraphy, *Boreas*, 32(2), 347-360.

Gunnarson, B. E., H. W. Linderholm, and A. Moberg (2011), Improving a tree-ring reconstruction from west-central Scandinavia: 900 years of warm-season temperatures, *Climate Dynamics*, 36(1-2), 97-108.

Gunnarson, B. E., T. Josefsson, H. W. Linderholm, and L. Östlund (2012), Legacies of pre-industrial land use can bias modern tree-ring climate calibrations, *Climate Research* (CR), 53(1), 63-76.

Hammarlund, D., G. Velle, B. B. Wolfe, T. W. Edwards, L. Barnekow, J. Bergman, S. Holmgren, S. Lamme, I. Snowball, and B. Wohlfarth (2004), Palaeolimnological and sedimentary responses to Holocene forest retreat in the Scandes Mountains, west-central Sweden, *The Holocene*, 14(6), 862-876.

Harris, I., P. Jones, T. Osborn, and D. Lister (2014), Updated high-resolution grids of monthly climatic observations–the CRU TS3. 10 Dataset, *International Journal of Climatology*, 34(3), 623-642.

Helama, S., M. Lindholm, M. Timonen, J. Meriläinen, and M. Eronen (2002), The supra-long Scots pine tree-ring record for Finnish Lapland: Part 2, interannual to centennial variability in summer temperatures for 7500 years. *The Holocene*, 12(6), 681-687.

Helama, S., B. W. Arentoft, O. Collin-Haubensak, M. D. Hyslop, C. K. Brandstrup, H. M. Mäkelä, Q. Tian, and R. Wilson (2013), Dendroclimatic signals deduced from riparian versus upland forest interior pines in North Karelia, Finland, *Ecological research*, 28(6), 1019-1028.

Helama, S., M. Vartiainen, J. Holopainen, H. M. Mäkelä, T. Kolström, and J. Meriläinen (2014), A palaeotemperature record for the Finnish Lakeland based on microdensitometric variations in tree rings. *Geochronometria*, 41(3), 265-277.

Holland, M. M., and C. M. Bitz (2003), Polar amplification of climate change in coupled models. *Climate Dynamics*, 21(3-4), 221-232.

Holmes, R. L. (1983), Computer-assisted quality control in tree-ring dating and measurement. *Tree-ring bulletin* 43(1), 69-78.

Huang, N. E., and Z. Wu (2008), A review on Hilbert-Huang transform: Method and its applications to geophysical studies, *Reviews of Geophysics*, 46(2), doi: 10.1029/2007RG000228.

Huang, N. E., Z. Shen, S. R. Long, M. C. Wu, H. H. Shih, Q. Zheng, N. C. Yen, C. C. Tung, and H. H. Liu (1998), The empirical mode decomposition and the Hilbert spectrum for nonlinear and non-stationary time series analysis, in *Proceedings of the Royal Society of London A: Mathematical, Physical and Engineering Sciences* (Vol. 454, No. 1971, pp. 903-995). The Royal Society.

Hurrell, J. W. (1995), Decadal trends in the North Atlantic Oscillation: regional temperatures and precipitation. *Science*, 269(5224), 676-679.

IPCC, 2013: Climate Change 2013: *The Physical Science Basis. Contribution of Working Group I to the Fifth Assessment Report of the Intergovernmental Panel on Climate Change* [Stocker, T.F., D. Qin, G.-K. Plattner, M. Tignor, S.K. Allen, J. Boschung, A. Nauels, Y. Xia, V. Bex and P.M. Midgley (eds.)]. Cambridge University Press, Cambridge, United Kingdom and New York, NY, USA, 1535 pp, doi:10.1017/CBO9781107415324.

Ji, F., Z. Wu, J. Huang, and E. P. Chassignet (2014), Evolution of land surface air temperature trend, *Nature Climate Change*, 4(6), 462-466.

Johannessen T. W. (1970), The climate of Scandinavia. Climates of Northern and Western Europe. *World survey of climatology*, 5: 23-80.

Johansson, B., D. Chen (2003), The influence of wind and topography on precipitation distribution in Sweden: Statistical analysis and modelling. *International Journal of Climatology*, 23(12), 1523-1535.

Jones, P. D., T. J. Osborn, and K. R. Briffa (2001), The evolution of climate over the last millennium. *Science*, 292(5517), 662-667.

Kerr, R. A. (2000), A North Atlantic climate pacemaker for the centuries, *Science*, (288), 1984-1985.

Lamb, H. H. (1969). Climatic fluctuations. *World survey of climatology*, 2, 173-249.

Linderholm, H. W., and B. E. Gunnarson (2005), Summer temperature variability in central Scandinavia during the last 3600 years, *Geografiska Annaler: Series A, Physical Geography*, 87(1), 231-241.

Linderholm, H., J. Björklund, K. Seftigen, B. E. Gunnarson, H. Grudd, J.-H. Jeong, I. Drobyshev, and Y. Liu (2010), Dendroclimatology in Fennoscandia–from past accomplishments to future potential, *Climate of the Past*, 6, 93-114.

Linderholm, H. W., P. Zhang, B. E. Gunnarson, J. Björklund, E. Farahat, M. Fuentes, E. Rocha, R. Salo, K. Seftigen, and P. Stridbeck (2014a), Growth dynamics of tree-line and lake-shore Scots pine (*Pinus sylvestris* L.) in the central Scandinavian Mountains during the Medieval Climate Anomaly and the early Little Ice Age, *Frontiers in Ecology and Evolution: Paleoecology*, 2, 20.

Linderholm, H. W., J. Björklund, K. Seftigen, B. E. Gunnarson, and M. Fuentes (2014b), Fennoscandia revisited: a spatially improved tree-ring reconstruction of summer temperatures for the last 900 years. *Climate Dynamics*, 1-15.

Ljungqvist, F. C. (2010), A new reconstruction of temperature variability in the extra-tropical Northern Hemisphere during the last two millennia. *Geografiska Annaler: Series A, Physical Geography*, 92(3), 339-351.

Ljungqvist, F., P. J. Krusic, G. Brattström, and H. S. Sundqvist (2012), Northern Hemisphere temperature patterns in the last 12 centuries, *Climate of the Past*, 8(1), 227-249.

Loader, N., G. Young, H. Grudd, and D. McCarroll (2013), Stable carbon isotopes from Torneträsk, northern Sweden provide a millennial length reconstruction of summer sunshine and its relationship to Arctic circulation, *Quaternary Science Reviews*, 62, 97-113.

Lundqvist, J. (1969), *Beskrivning till jordartskarta över Jämtlands län: 4 Karten. Kt*, Sveriges Geologiska Undersökning.

Luterbacher, J., E. Xoplaki, D. Dietrich, P. Jones, T. Davies, D. Portis, J. Gonzalez-Rouco, H. Von Storch, D. Gyalistras, and C. Casty (2001), Extending North Atlantic oscillation reconstructions back to 1500, *Atmospheric Science Letters*, 2(1-4), 114-124.

Mann, M. E., R. S. Bradley, and M. K. Hughes (1999), Northern hemisphere temperatures during the past millennium: inferences, uncertainties, and limitations. *Geophysical research letters*, 26(6), 759-762.

Mann, M. E., Z. Zhang, M. K. Hughes, R. S. Bradley, S. K. Miller, S. Rutherford, and F. Ni, (2008), Proxy-based reconstructions of hemispheric and global surface temperature variations over the past two millennia. *Proceedings of the National Academy of Sciences*, 105(36), 13252-13257.

Mann, M. E., Z. Zhang, S. Rutherford, R. S. Bradley, M. K. Hughes, D. Shindell, C. Ammann, G. Faluvegi, and F. Ni (2009), Global signatures and dynamical origins of the Little Ice Age and Medieval Climate

Anomaly. *Science*, 326(5957), 1256-1260.

Matskovsky, V. V., and S. Helama (2014), Testing long-term summer temperature reconstruction based on maximum density chronologies obtained by reanalysis of tree-ring data sets from northernmost Sweden and Finland. *Climate of the Past*, 10(4), 1473-1487.

McCarroll, D., N. J. Loader, R. Jalkanen, M. H. Gagen, H. Grudd, B. E. Gunnarson, A. J. Kirchhefer, M. Friedrich, H. W. Linderholm, and M. Lindholm (2013), A 1200-year multiproxy record of tree growth and summer temperature at the northern pine forest limit of Europe, *The Holocene*, doi: 10.1177/0959683612467483.

Melvin, T. M. (2004), Historical growth rates and changing climatic sensitivity of boreal conifers, PhD Thesis, University of East Anglia.

Melvin, T. M., and K. R. Briffa (2008), A "signal-free" approach to dendroclimatic standardisation, *Dendrochronologia*, 26(2), 71-86.

Melvin, T. M., H. Grudd, and K. R. Briffa (2013), Potential bias in 'updating' tree-ring chronologies using regional curve standardisation: Re-processing 1500 years of Torneträsk density and ring-width data. *The Holocene*, 23(3), 364-373.

Melvin, T. M., and K. R. Briffa (2014a), CRUST: Software for the implementation of regional chronology standardisation: Part 1. Signal-free RCS, *Dendrochronologia*, 32(1), 7-20.

Melvin, T. M., and K. R. Briffa (2014b), CRUST: Software for the implementation of Regional Chronology Standardisation: Part 2. Further RCS options and recommendations, *Dendrochronologia*, 32(4), 343-356.

Moberg, A., H. Bergström, J. R. Krigsman, and O. Svanered (2002), Daily air temperature and pressure series for Stockholm (1756–1998), in *Improved Understanding of Past Climatic Variability from Early Daily European Instrumental Sources*, edited, pp. 171-212, Springer.

Moberg, A., D. M. Sonechkin, K. Holmgren, N. M. Datsenko, and W. Karlén (2005), Highly variable Northern Hemisphere temperatures reconstructed from low-and high-resolution proxy data, *Nature*, 433(7026), 613-617.

PAGES 2k Consortium (2013), Continental-scale temperature variability during the last two millennia. *Nature Geoscience*, 6, 339-346, doi:10.1038/ngeo1797.

Parmesan, C., and G. Yohe (2003), A globally coherent fingerprint of climate change impacts across natural systems. *Nature*, 421(6918), 37-42.

Patz, J. A., D. Campbell-Lendrum, T. Holloway, and J. A. Foley (2005), Impact of regional climate change on human health. *Nature*, 438(7066), 310-317.

Rocha, E. (2014), June-Junly summer temperature reconstruction in central Scandinavia over the past two millennia inferred from Norway spruce tree ring width chronology. Master thesis, University of Gothenburg.

Rodwell, M., and C. Folland (2002), Atlantic air–sea interaction and seasonal predictability, *Quarterly Journal of the Royal Meteorological Society*, 128(583), 1413-1443.

Rodwell, M., D. Rowell, and C. Folland (1999), Oceanic forcing of the wintertime North Atlantic Oscillation and European climate, *Nature*, 398(6725), 320-323.

Rogers, J. C. (1997), North Atlantic storm track variability and its association to the North Atlantic Oscillation and climate variability of northern Europe. *Journal of Climate*, 10(7), 1635-1647.

Salo, R. (2014), 760-years of summer sunshine variation in the central Scandinavian Mountains, as inferred from tree-ring stable carbon isotopes. Master thesis, University of Gothenburg.

Santer, B. D., T. M. L. Wigley, J. S. Boyle, D. J. Gaffen, J. J. Hnilo, D. Nychka, D. E. Parker, and K. E. Taylor (2000), Statistical significance of trends and trend differences in layer-average atmospheric temperature time series. *Journal of Geophysical Research: Atmospheres (1984–2012)*, 105(D6), 7337-7356.

Schneider, S. H., and C. Mass (1975), "Volcanic dust, sunspots, and temperature trends", *Science*, 190, 741-746.

Schurer, A. P., S. F. Tett, and G. C. Hegerl (2014), Small influence of solar variability on climate over the past millennium. *Nature Geoscience*, 7(2), 104-108.

Schweingruber, F. H. (1996), *Tree rings and environment: dendroecology*. Paul Haupt AG Bern.

Schweingruber, F., L. Kairiukstis, and S. Shiyatov (1990), Sample selection, Methods of dendrochronology: Applications in the environmental sciences, 23-35.

Schweingruber, F., H. Fritts, O. Bräker, L. Drew, and E. Schär (1978), The X-ray technique as applied to dendroclimatology, *Tree-ring Bull* 38, 61–91.

Seftigen, K., J. Björklund, E. R. Cook, and H. W. Linderholm (2014), A tree-ring field reconstruction of Fennoscandian summer hydroclimate variability for the last millennium, *Climate Dynamics*, 44, 11-12, 3141-3154.

Seppä, H., A. Bjune, R. Telford, H. Birks, and S. Veski (2009), Last nine-thousand years of temperature variability in Northern Europe, *Climate of the Past*, 5(3), 523-535.

Servonnat J., P. Yiou, M. Khodri, D. Swingedouw, S. Denvil (2010), Influence of solar variability CO2 and orbital forcing between 1000 and 1850 AD in the IPSLCM4 model. *Climate of the Past*, 6, 445–460.

Shindell, D. T., G. A. Schmidt, M. E. Mann, D. Rind and A. Waple (2001), Solar forcing of regional climate change during the Maunder Minimum. *Science* 294, 2149–2152.

Shindell, D. T., G. A. Schmidt, R. L. Miller, and M. E. Mann (2003), Volcanic and solar forcing of climate change during the preindustrial era. *Journal of Climate*, 16(24), 4094-4107.

Steinhilber, F., J. A. Abreu, J. Beer, I. Brunner, M. Christl, H. Fischer, U. Heikkilä, P. W. Kubik, M. Mann, and K. G. McCracken (2012), 9,400 years of cosmic radiation and solar activity from ice cores and tree rings, *Proceedings of the National Academy of Sciences*, 109(16), 5967-5971.

Stuiver, M., and P. D. Quay (1980). Changes in atmospheric carbon-14 attributed to a variable sun. *Science*, 207(4426), 11-19.

Sundqvist, H. S., K. Holmgren, A. Moberg, C. Spoetl, and A. Mangini (2010), Stable isotopes in a stalagmite from NW Sweden document environmental changes over the past 4000 years, *Boreas*, 39(1), 77-86.

Sutton, R. T., and D. L. Hodson (2005), Atlantic Ocean forcing of North American and European summer climate. *Science*, 309(5731), 115-118.

Sutton, R. T., and B. Dong (2012), Atlantic Ocean influence on a shift in European climate in the 1990s. *Nature Geoscience*, 5(11), 788-792.

Taylor, K. E., R. J. Stouffer, and G. A. Meehl (2012), An overview of CMIP5 and the experiment design, *Bulletin of the American Meteorological Society*, 93(4), 485-498.

Torrence, C., and G. P. Compo (1998), A practical guide to wavelet analysis, *Bulletin of the American Meteorological society*, 79(1), 61-78.

Travis, D. J., V. Meentemeyer, and R. P. Belanger (1990), Stressed trees produce a better climatic signal than healthy trees, *Tree-Ring Bulletin*, 50, 29-32.

Trouet, V., J. Esper, N. E. Graham, A. Baker, J. D. Scourse, and D. C. Frank (2009), Persistent positive

North Atlantic Oscillation mode dominated the medieval climate anomaly, S*cience*, 324(5923), 78-80.

Tuomenvirta, H., Drebs, A., Forland E., Tveito, O. E., Alexandersson, H., Laursen, E. V., and Jonsson, T. (2001), Nordklim data set 1.0 - description and illustrations, *DNMI Report*, 8, 1-26.

Ulbrich, U., and M. Christoph (1999), A shift of the NAO and increasing storm track activity over Europe due to anthropogenic greenhouse gas forcing. *Climate dynamics*, 15(7), 551-559.

Walker G. T., and E. W. Bliss (1932), World weather, *V. Mem R Meteorol Soc* 4, 53–84.

Weng, H., and K. M. Lau (1994), Wavelets, period doubling, and time-frequency localization with application to organization of convection over the tropical western Pacific. *Journal of the atmospheric sciences*, 51(17), 2523-2541.

Wigley, T. M., K. R. Briffa, and P. D. Jones (1984), On the average value of correlated time series, with applications in dendroclimatology and hydrometeorology, *Journal of Climate and Applied Meteorology*, 23(2), 201-213.

Wigley, T. M. L., P. D. Jones, and K. R. Briffa (1987), Cross-dating methods in dendrochronology. *Journal of Archaeological Science*, 14(1), 51-64.

Wu, Z., and N. E. Huang (2009), Ensemble empirical mode decomposition: a noise-assisted data analysis method, *Advances in adaptive data analysis*, 1(01), 1-41.

Young, A. B., D. M. Cairns, C. W. Lafon, J. Moen, and Martin, L. E. (2011), Dendroclimatic relationships and possible implications for mountain birch and Scots pine at treeline in northern Sweden through the 21st century This article is a contribution to the series Tree recruitment, growth, and distribution at the circumpolar forest-tundra transition. *Canadian Journal of Forest Research*, 41(3), 450-459.

Young, G. H., D. McCarroll, N. J. Loader, M. H. Gagen, A. J. Kirchhefer, and J. C. Demmler (2012), Changes in atmospheric circulation and the Arctic Oscillation preserved within a millennial length reconstruction of summer cloud cover from northern Fennoscandia, *Climate dynamics*, 39(1-2), 495-507.

Zachrisson, O., M. C. Nilsson, I. Steijlen, and G. Hornberg (1995), Regeneration pulses and climate-vegetation interactions in nonpyrogenic boreal Scots pine stands. *Journal of Ecology*, 469-483.

Zhang, X., A. Sorteberg, J. Zhang, R. Gerdes, and J. C. Comiso (2008), Recent radical shifts of atmospheric circulations and rapid changes in Arctic climate system. *Geophysical Research Letters*, 35(22), doi: 10.1029/2008GL035607.